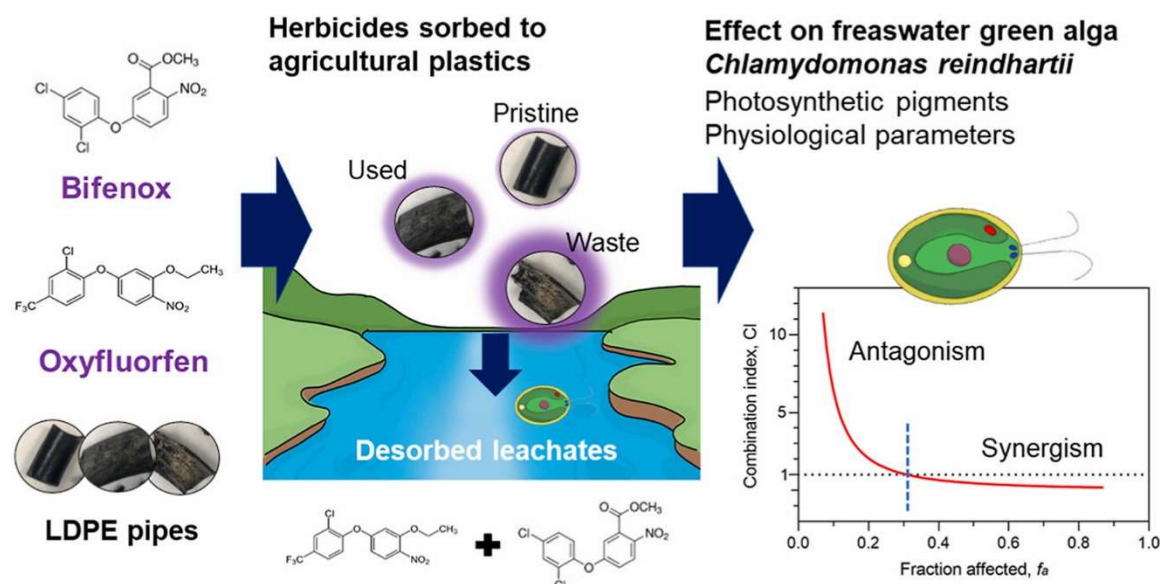


Leaching of herbicides mixtures from pre-exposed agricultural plastics severely impact microalgae

Please, cite as follows:

Irene Verdú, Miguel González-Pleiter, Francisco Leganés, Francisca Fernández-Piñas, Roberto Rosal. Leaching of herbicides mixtures from pre-exposed agricultural plastics severely impact microalgae. *Chemosphere* 326, 138475, 2023.

<https://doi.org/10.1016/j.chemosphere.2023.138475>



<https://www.sciencedirect.com/science/article/pii/S0045653523007427>

Leaching of herbicides mixtures from pre-exposed agricultural plastics severely impact microalgae

Irene Verdú¹, Miguel González-Pleiter¹, Francisco Leganés^{1,2}, Francisca Fernández-Piñas^{1,2}, Roberto Rosal^{3,*}

¹ Department of Biology, Faculty of Science, Universidad Autónoma de Madrid, E-28049, Madrid, Spain

² Department of Chemical Engineering, Universidad de Alcalá, E-28871, Alcalá de Henares, Madrid, Spain

³ Centro de Investigación en Biodiversidad y Cambio Global (CIBC-UAM), Universidad Autónoma de Madrid, Darwin 2, 28049, Madrid, Spain

* Corresponding author: roberto.rosal@uah.es

Abstract

Farmlands represent a source of aged plastics and pesticides to the surrounding environments. It has been shown that chemicals can be sorbed and desorbed from plastics, but the interaction between plastic and mixtures of pesticides and their effects on freshwater biota has not been assessed yet. The aim of the work was to assess the potential role of agricultural plastics as vectors for a mixture of two herbicides and the impact of the herbicide mixture leached from them towards the freshwater microalga *Chlamydomonas reinhardtii*. Pristine and aged polyethylene plastics collected from agricultural areas were exposed to the herbicides, bifenox, oxyfluorfen and their mixtures. The microalgae were exposed for 72 h to the leachates desorbed from plastics and the effect was quantified in terms of total chlorophyll content and several physiological parameters assessed by flow cytometry. Our results showed that changes in physicochemical properties (hydroxyl and carbonyl index, hydrophobicity, texture) in aged plastics increased their capacity to retain and to desorb the herbicides. Microalgae exposed to leachates containing bifenox, oxyfluorfen, or their mixture showed reactive oxygen species overproduction, lipid peroxidation, membrane potential hyperpolarization, intracellular pH acidification, and a loss of metabolic activity. The toxicological interactions of the leachate mixture were assessed using the Combination Index (CI)-isobologram method showing antagonism at low effect levels turning to synergism when the effect increased. In this work, we proved the hypothesis that ageing increases the capacity of agricultural plastics to behave as vector for toxic chemicals to the biota.

Keywords: Agricultural plastics; Bifenox; Oxyfluorfen; Microalgae; Mixture toxicity; Pollutant vectors

1. Introduction

Agriculture is a major plastic consumer. The increased demand driven by population growth and the needs of modern society result in an intense use of plastic in search for earlier productions, higher crop yields, improved food quality, and lower water consumption (Cusworth et al., 2022). Plasticulture along with irrigation with reclaimed water and the use of sewage sludge as soil amendment, represent the main inputs of plastic to agroecosystems (Zhou et al., 2020; Edo et al., 2022). Agricultural plastics are subject to weathering processes, which break them down into small pieces, known as microplastics (MPs) if their larger dimension is < 5 mm. The available data on the concentration of MPs in agroecosystems is still scarce, but it has been estimated that between 44,000 and 430,000 tons of MPs enter annually the farmlands in Europe and North America (Nizzetto et al., 2016). The contamination of soil ecosystems by MPs is expected to be high in view of their intense use and limited mobility, but plastic fragments can also be transported from soils to freshwater by run-off (Rehm et al., 2021). The available studies reported that polyolefins are the most commonly detected plastics in soils and aquatic

environments in agreement with their prevalence in agricultural uses (Piehl et al., 2018).

Plastic may exert negative effects as vector for sorbed chemicals, an effect frequently discussed because of the capacity of plastics to concentrate pollutants, which can be eventually released (Hartmann et al., 2017; González-Pleiter et al., 2021; Fajardo et al., 2022). Besides, natural processes such as the aging of MPs could change these sorption and desorption behaviors as reported elsewhere (Liu et al., 2019). Farmlands are the main source of pesticides to the environment. It has been demonstrated that MPs can sorb the pesticides used in agriculture (Gong et al., 2019; Zhang et al., 2021). Nerín et al. (1996) observed slow, but thermodynamically favored sorption of the currently used pesticides onto low-density polyethylene (LDPE) and ethylene vinyl acetate films. Wang et al. (2020) and Lan et al. (2021) reported the sorption capacity of polyethylene (PE) agricultural films for common pesticides. However, chemicals in the environment occur in mixtures. (Lundqvist et al., 2019). Little attention has been paid to mixtures in plastic sorption-desorption studies, which can differ in behavior with respect to single-chemical systems (Ho and Leung, 2019).

Two diphenyl-ether herbicides, bifenoxy (BIF) and oxyfluorfen (OXY), are currently in wide use. Both act by inhibiting the enzyme protoporphyrinogen oxidase (Protox) that mediates the transformation of protoporphyrinogen IX into protoporphyrin IX, the necessary precursor for chlorophyll and heme synthesis (Grossmann, 2005). Diphenyl-ether herbicides, due to their low volatility and hydrophobicity are relatively persistent in soils where they can be phytotoxic for months (Székács, 2021). Besides, diphenyl ethers are metabolized by slow cleavage of the ether bond followed by conjugation of nitrophenyl to cysteine or glutathione. Their decomposition due to microbial assimilation or photochemical reactions is slow. BIF has been included in the list of priority substances (Annex II) of the Water Framework Directive as revised by Directive (2013)/39/EU. Peris et al. (2022) detected the presence of 5.0–25.4 ng/g (dry weight) of OXY in sediments from the Ebro River basin due to run-off from nearby agricultural areas. In river water, Ibrahim and Sayed (2019) detected concentrations as high as 23.6 mg/L of OXY in some tributaries of the Nile River. Likewise, BIF has been detected in different water surfaces at concentrations in the 0.16–4.80 µg/L range (EFSA, 2007).

The use of herbicides is complex and depends on soil type, climatic factors, application period, and type of use (pre- or post-emergence), among others. Besides, resistances are common and sequential applications or the use of different compounds with the same of different mode of action is usual even in the same culture campaign to allow better weed control (Comont et al., 2020). Moreover, neighboring plots can use different chemicals, so that cross-transference is a commonly found scenario. The exposure of non-target species may take place after application episodes, but spreads in time due to the buffering capacity of soil and to their retention on other materials they may find in their way when swept along with irrigation of rainwater. The migration of chemicals from their point of application in agricultural lands, to rivers, lakes and reservoirs is well documented and represents a major concern not only for ecosystems, but to the human health.

Microalgae is one of the non-target groups of primary producers typically exposed to pesticides. They are at the base of the aquatic trophic chain and represent more than 50% of the global oxygen production and carbon fixation. Among them, *Chlamydomonas reinhardtii* is a well-studied green microalga commonly used in ecotoxicology because of its high sensitivity to a wide range of contaminants. Microalgae as primary producers are at the base of freshwater ecosystems and any impairment would be transmitted to zooplankton and the rest of the trophic chain. It is expected that microalgae, as non-target organisms, will be exposed to a variety of chemicals. The fact that plastic can retain pesticides makes combined exposure more likely

because chemicals from different applications could co-occur.

Specifically, the aim of this research is to assess the role of agricultural plastics as vectors for herbicide mixtures, a topic that has received little attention to date, and to explore the joint effect of BIF and OXY to *C. reinhardtii*. For it, pristine and environmentally aged agricultural plastics (LDPE plastic pipes) were put in contact with BIF and OXY, in single and combined exposure; subsequently, the freshwater microalga *C. reinhardtii* was exposed to herbicides leachates from pre-exposed plastics and the effect on photosynthetic pigments and metabolic activities was recorded. To our knowledge, this is the first study showing the sorption and desorption of a pesticide mixture in naturally aged plastic and its effect to a non-target organism.

2. Materials and methods

2.1. Materials and chemicals

Pristine and aged low-density polyethylene plastic pipes (PE32-LDPE, 16 mm outside diameter, wall thickness 1.2 mm) in common use for water pipping were obtained from an agricultural area in Southeast Spain (Fig. S1, Supplementary Material, SM). Pristine plastics were acquired from a local agricultural retailer. Aged plastics were collected from two sites, one while still in use in a farmland and the other as abandoned waste in a seasonally dry riverbed close to the farmland. Plastic samples were carefully washed several times with distilled water, dried at room temperature (25 °C) and cut with a stainless-steel blade into 2 × 1.8 mm pieces. The materials were denoted as “P”, “U” and “R” corresponding to pristine, in use and residual tubes, respectively. The plastics were kept in darkness and stored in amber glass flasks at 4 °C until further characterization and use.

Bifenoxy (BIF; Methyl 5-(2,4-dichlorophenoxy)-2-nitrobenzoate, C₁₄H₉Cl₂NO₅, CAS: 42,576-02-3, ≥ 98.0%) and Oxyfluorfen (OXY; 2-chloro-1-(3-ethoxy-4-nitrophenoxy)-4-(trifluoromethyl) benzene; C₁₅H₁₁ClF₃NO₄; CAS number 42874-03-3; ≥ 98.0%) were acquired from Sigma-Merck. Stock solutions (20,000 µg/mL) were prepared in dimethyl sulfoxide and methanol and stored in amber flasks at 4 °C and –20 °C, respectively. The physicochemical properties of BIF and OXY are shown in Table S1 (SM). The content of dimethyl sulfoxide and methanol in working was kept <0.05% (v/v) to avoid cosolvent toxic effects (Pinal et al., 1990).

2.2. Plastics characterization

The functional groups on the outer plastic surface were determined using Attenuated Total Reflectance Fourier-Transform Infrared Spectroscopy (ATR-FTIR). Three replicates were performed using a Thermo Scientific Nicolet iS10 apparatus equipped with Smart iTR-Diamond module. OMNIC 8.3 software was used to process spectra in the 4000–550 cm⁻¹ range with a

resolution of 8 cm^{-1} and 32 scans. FTIR measurements allowed determining hydroxyl and carbonyl indexes according to the following expressions (Brandon et al., 2016; Zvekić et al., 2022).

$$\text{Hydroxyl index} = \frac{\text{Maximum absorbance (3300–3400 cm}^{-1}\text{)}}{\text{Absorbance (2920 cm}^{-1}\text{)}} \quad [1]$$

$$\text{Carbonyl index} = \frac{\text{Absorbance area (1505–1855 cm}^{-1}\text{)}}{\text{Absorbance area (1465–1497 cm}^{-1}\text{)}} \quad [2]$$

The features of plastics surface were assessed by Scanning electron microscopy (SEM) using a JSM-IT500 (JEOL InTouchScope™ series) microscope operating at 15 kV on gold sputter-coated samples. The microtexture of plastic materials was examined by 3D optical profiling, using a 3D surface microscope Leica DCM8. Representative images were analyzed by LeicaScan software (6.1 version) to obtain the ratio of surface area to projected surface (*Sdr*). The kurtosis value (*Sk*) was obtained as a measure of the sharpness of the roughness profile (Blunt and Jiang, 2033). Three replicates per sample were performed. Surface hydrophobicity was measured by water contact angle (WCA), using a DSA25 Krüss Analyzer. The thermal properties of plastic materials, namely glass transition temperature (T_g), melting point (T_m), and crystallinity were determined using differential scanning calorimetry (DSC) in a DSC apparatus SDT Q600 from TA Instruments with heating rate 10 °C/min between -100 and 200 °C . The percentage of crystallinity, $X(\%)$, was calculated from the ratio of the melting enthalpy of the sample and the melting enthalpy of a fully crystalline polymer (290 kJ/kg for PE).

2.3. Sorption-desorption experiments

The materials P, U, and R with a concentration of 100 particles/L were exposed to $400\text{ }\mu\text{g/L}$ of BIF, $54\text{ }\mu\text{g/L}$ of OXY, and their mixture, MIX ($400\text{ }\mu\text{g/L}$ and $54\text{ }\mu\text{g/L}$) in 30 mL of phosphate buffer (K_2HPO_4 0.011 mg/L and KH_2PO_4 0.054 mg/L) adjusted at pH 6.5 ($493.3 \pm 3.8\text{ }\mu\text{S/cm}$) for 24 h. These concentrations were selected because they are close to their respective water solubility and about EC_{80} for chlorophyll content of *C. reinhardtii*, which was selected as the main toxicological endpoint (Table S1, SM). At these chosen concentrations, sorption and desorption could be accurately quantified by HPLC/MS as well as the biological effect of leachates as indicated below. The plastic suspensions were kept in a rotary shaker at 140 rpm and 25 °C in darkness to avoid potential herbicide photodegradation. Then, plastic fragments were collected and centrifuged (4300 rpm) for 30 s to remove the adhered liquid as indicated elsewhere (Verdú et al., 2021). Supernatant samples from each sorption treatment were taken and stored for chemical analyses. Subsequently, the herbicide-loaded plastics were put into a clean phosphate buffer for 24 h to allow the desorption of herbicides. Plastic controls (P, U, and R non-exposed to the herbicides) were analyzed to assess for the possible presence of sorbed pesticides in

materials exposed to the environment (U and R). Herbicide controls (BIF, OXY, and MIX without plastic fragments) were also checked for possible pesticide degradation or their sorption onto the glass vessels. Supernatant samples from each sorption treatment, the leachates desorbed from the preloaded plastics, and controls, were analyzed by HPLC. Each sorption-desorption experiment was performed in triplicate. A scheme of the complete experimental design is given in Fig. S2 (SM).

2.4. Chemical analyses

The quantification of BIF and OXY in sorption and desorption experiments, applied singly and in mixture, was performed by high-pressure liquid chromatography (Agilent HPLC 1200) coupled to a mass analyzer (triple quadrupole Agilent 6410B). A C18, $2\text{ }\mu\text{m}$ particle size, $100 \times 3.0\text{ mm}$ ACE EXCEL 2 column was used for the chromatographic separation. The mobile phase consisted of 0.1% of formic acid in Milli-Q water (eluent A) and acetonitrile (ACN) (eluent B) at a flow rate of 0.3 mL/min using a gradient as follows: 70 % (A) and 30 % (B), 5 min; 100 % (B) from 5 to 10.2 min; followed by 70 % (A) and 30 % (B) until 15 min. The injection volume was $10\text{ }\mu\text{L}$. The column temperature was 40 °C . The sorbed concentrations of the herbicides were expressed as mass of herbicide per unit mass of plastic ($\mu\text{g/g}$), whereas desorbed concentrations were expressed as mass of herbicide per unit volume of liquid ($\mu\text{g/L}$).

2.5. Bioassays

The unicellular green microalga, *Chlamydomonas reinhardtii* was obtained from the Culture Collection of Algae and Protozoa of Dunstaffnage Marine Laboratory (Scotland, UK) and routinely cultured in TAP culture medium diluted 6 times (TAP/6) in a rotary shaker, at 140 rpm and 25 °C under continuous light of $50\text{ }\mu\text{mol photons m}^{-2}\text{ s}^{-1}$. Cells in exponential growth phase were diluted in 1 mL of 10-fold concentrated TAP/6 and 8.5 mL of the leachates obtained from desorption experiments. The initial $\text{OD}_{750\text{nm}}$ was 0.2 (5×10^5 cells/mL). Microalgae were exposed for 72 h to (1) leachates from P, U, and R not exposed to herbicides), (2) leachates from plastics pre-exposed to BIF (BIF-P, BIF-U, BIF-R); (3) leachates from plastics pre-exposed to OXY (OXY-P, OXY-U, OXY-R), and (4) leachates from plastics pre-exposed to the mixture BIF+OXY (MIX-P, MIX-U, MIX-R). To toxicity of the herbicides at the same concentration measured from leachates was also tested. In what follows, these treatments are denoted as dBIF-P/U/R, dOXY-P/U/R, and dMIX-P/U/R. Microalgae non-exposed to the herbicides were used as controls. Six replicates of controls and three replicates of every treatment were carried out. After 72 h of exposure, the total content of chlorophyll (Chl *a* + Chl *b*) was measured. Total chlorophyll content was selected as the main endpoint because the impairment of their synthesis is the mode of action of both pesticides. For it, the photosynthetic pigments were

extracted in acetone (90 %) at 4 °C for 24 h in darkness, and the absorbance at 664 and 647 nm for chl *a* and chl *b*, respectively was measured. The concentration of chlorophylls was determined according to Jeffrey and Humphrey (1975).

The nature of the toxicological interaction of BIF and OXY (additive, synergistic or antagonistic) was assessed by means of the combination index (CI)-isobologram method (Chou, 2010). For each level of effect (f_a), the CI can be calculated according to the following equation:

$$(CI)_x^n = \sum_{j=1}^n \frac{D_j}{(D_x)_j} = \sum_{j=1}^n \frac{(D_x)_{1-n} \left(\frac{D_j}{\sum_1^n D} \right)}{(D_m)_j \left[\frac{(f_{ax})_j}{1-(f_{ax})_j} \right]^{m_j}} \quad [3]$$

D is the concentration of toxicant, D_m the concentration that corresponds to a 50% affected fraction (f_a) (or EC_{50}), m is the shape coefficient of the dose-effect curve, f_u the fraction unaffected ($f_u = 1 - f_a$) and $(CI)_x^n$ is the CI of n chemicals (in mixture) for any given f_a . The evaluation of CI requires computing the sum of doses that exert a certain inhibition for the endpoint under study, $(D_x)_{1-n}$; the proportion of the dose of each compound that produces the same effect, $(D_j/\sum_1^n D)$; and the dose of each compound that exerts the same effect by itself, which is the denominator in both summations. The computation of CI can be performed by means of Compusyn software (Chou and Martin, 2007). A value of $CI = 1$ means additivity, while $CI < 1$ represents synergism and $CI > 1$ antagonism.

The effect of the leachates released from plastic fragments pre-exposed to BIF, OXY and their mixture on the physiologic parameters of microalgae was assessed by flow cytometry in a Beckman Coulter Cytoflex S apparatus. In addition to size, complexity, and chlorophyll autofluorescence, five physiological parameters were measured using the fluorochromes specified in Table S2 (SM). They were: dihydrorhodamine 123 (DHR 123) for the detection of intracellular reactive oxygen species (ROS); C4, C9-BODIPY® for lipid peroxidation; bis-(1,3-dibutylbarbituric acid) trimethine oxonol, DiBAC₄(3), to determine the changes in cytoplasmic membrane potential; fluorescein diacetate, FDA, for cell metabolic activity; and 20,70-bis(2-carboxyethyl)-5(6)-carboxyfluorescein, BCECF-AM, for intracellular pH. The cells were incubated with the fluorochromes at room temperature. CytExpert software (Beckman) was used for image and data acquisition and processing. All measurements were normalized to cell size (FS detector) because cell volume can alter fluorescence emission. Fluorescence was analyzed in logarithmic mode and at least 10^4 gated cells were evaluated. Three independent experiments with six (control) and three

samples by treatment were carried out for each parameter.

2.6. Statistical data treatment

To assess statistical significance one-way ANOVA, and post-hoc comparisons following Tukey's HSD test were performed. Prior to it, the parametric assumptions of normality and homoscedasticity were checked by means of Shapiro-Wills and Levene tests. Spearman's rank correlation analysis was performed to determine the relationship between plastic characteristics and the sorption and desorption of herbicides. In all cases, differences were considered significant for a significance level of 0.05.

3. Results and discussion

3.1. Characterization of plastics

The FTIR spectra of the plastic materials are presented in Fig. 1A. All of them were clearly identified as PE based on the peaks corresponding to stretching vibrations of $-CH_2$ at 2914 cm^{-1} and 2847 cm^{-1} , the bending mode of $-CH_2$ at 1465 cm^{-1} , and the $-CH_2$ rocking vibration at 718 cm^{-1} . A peak with lower intensity was observed at 875 cm^{-1} , which could be assigned to $CaCO_3$, an additive widely used as filler in PE and other resins. Additional absorptions appeared at 1025 cm^{-1} in U and at 1025 cm^{-1} , 1649 cm^{-1} , and 3335 cm^{-1} in R, which can be assigned to C–O, C=O, and O–H stretching vibrations respectively, in all cases indicating oxidative weathering (Sorasan et al., 2021). A clear increase of hydroxyl and carbonyl indexes (Eqs. [1], [2]) was observed in samples U and R with respect to P (Table S3, SM). SEM photographs revealed the presence of cracks in U and R, notably more intense in R, indicating surface alteration upon exposed to the environment (Fig. 1-B, C, and D). These observations agree with texture values Sdr and Sku and 3D micrographs (Fig. 1-E, F, and G). The results showed that Sdr notably increased in U and R with respect to P. These results agree the evolution expected for polymers subject to photooxidative degradation (Cai et al., 2018; Jiang et al., 2018).

No changes were observed in crystallinity and Tg. A slight decrease was found for Tm in plastics R and U compared to the pristine material, P, as shown in Fig. 1H. These results agreed with previous research on the weathering of PE exposed to photodegradation (ter Halle et al., 2017; Sorasan et al., 2022). On the contrary, other authors indicated a progressive crystallinity increase upon mechanical and thermal oxidation attributed to the higher susceptibility of the amorphous phase to photooxidation (Feng et al., 2022). The inconclusive results on crystallinity could be attributed to the difficulty of evaluating the structural modifications suffered by PE upon aging (Carrasco et al., 2001).

Water Contact Angle (WCA) was used as a measure of surface hydrophobicity. As observed in Fig. 1-I, J, and

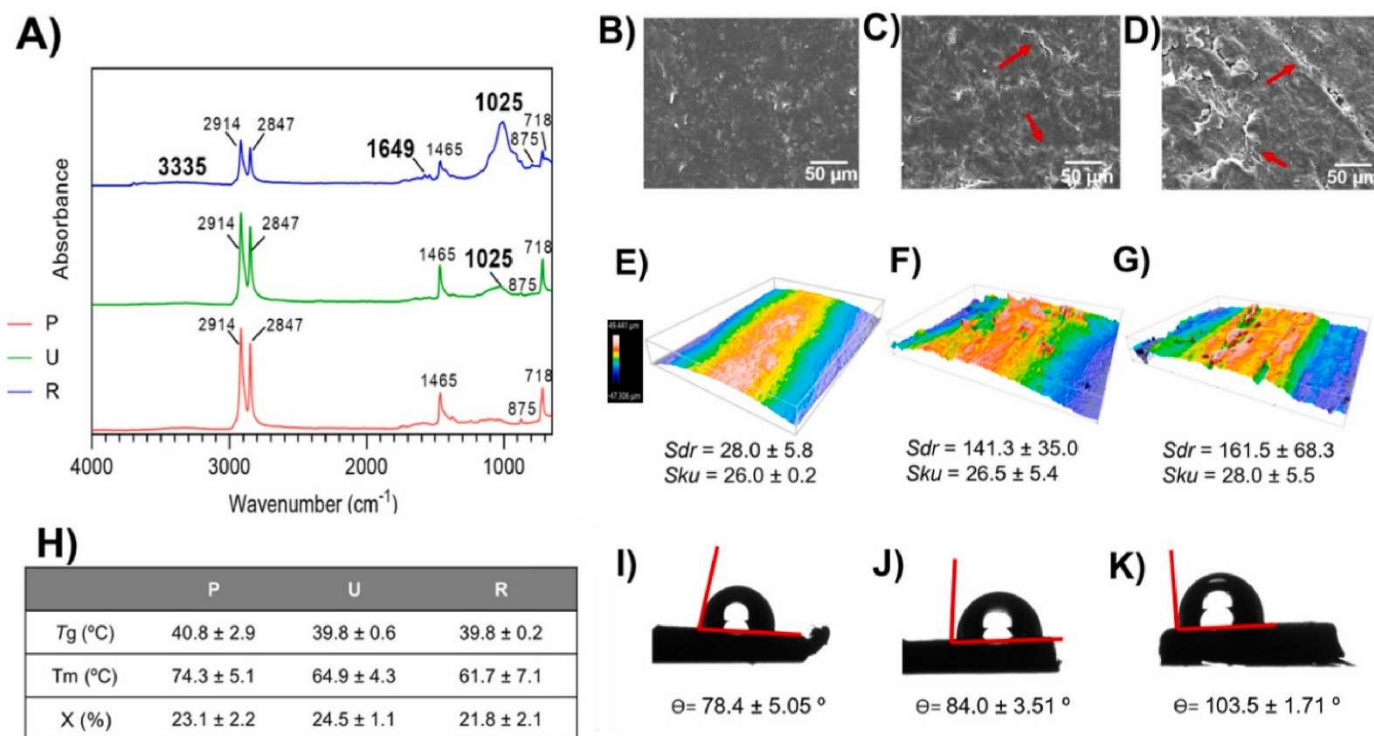


Figure 1. Physicochemical characterization of plastics (pristine, P, from a farmland, U, and from a dry riverbed, R). A) ATR-FTIR spectra. B-C-D) SEM images with red arrows marking cracks. E-F-G) Sdr and Skr values and 3D micrographs. H) T_g , T_m and X(%) obtained from DCS. I-J-K) WCA. P plastics correspond to figures B, E, and I); U plastics to C, F, and J); and R plastics to D, G, and K). .

K, WCA increased in U and even more in R with respect to P. Some studies reported lower hydrophobicity upon aging because of the generation of oxygen-containing groups (Feng et al., 2022). However, WCA is not solely determined by surface chemistry, but also by surface roughness, which can promote water repellency (McHale et al., 2005). This phenomenon can be explained because of surface resistance to wetting due to the air trapped in the cracks and pores between water drop and surface. Our results were consistent with the higher roughness observed in aged specimens (Fig. 1G) probably indicating that surface texture predominates over surface chemistry when determining the apparent hydrophobicity measured by WCA (Lin et al., 2022).

3.2. Sorption and desorption experiments

Fig. 2 shows the amount of BIF, OXY and their mixture (BIF + OXY) sorbed onto P, U, and R plastics as well as their respective concentration in the medium after desorption experiments. Significant differences are indicated by different letters and the same information expressed in percentages is shown in Fig. S3 (SM). The results showed that BIF was preferentially sorbed in R ($p < 0.05$), when exposed both individually and in mixture with OXY (BIF + OXY). OXY was also more sorbed in R, although the differences were lower and only significant with respect to P in individual exposure. The higher sorption of pollutants in aged MPs has been previously reported (Wu et al., 2020; You et al., 2021). The explanation is that the presence

of oxygen-containing groups, higher surface, and increased hydrophobicity led to higher sorption capacity. Table S4 (SM) presents the linear correlations between physicochemical parameters and chemical sorption results. A positive correlation for the sorbed amounts of both herbicides was obtained with hydroxyl and carbonyl indexes, roughness (sdr), and hydrophobicity (WCA). The non-polar character of both herbicides is expected to favor the interaction with hydrophobic surfaces. In addition, the expected formation of hydrogen bonds between oxygen-containing surface groups and the polar moieties of pesticides could explain their higher interaction with aged plastics.

In this work, no clear evidence was found that the sorption of one compound affected the other when both were present simultaneously in the same medium. Up to date, little is known about the competitive sorption of chemicals onto plastics and microplastics. It has been suggested that competing solutes could limit the accessibility to sorption sites (Bakir et al., 2012). The slight tendency of BIF to be more sorbed in the presence of OXY, would agree with others' results indicating enhanced sorption in competitive scenarios due to solute-solute interactions (Ho and Leung, 2019). In our case, the higher log K_{ow} value of OXY could increase BIF sorption due to hydrophobic interactions.

Concerning desorption, Fig 2B and Fig. S3 (SM) show that the desorbed amount of both compounds was higher in the case of plastic P compared to plastics U

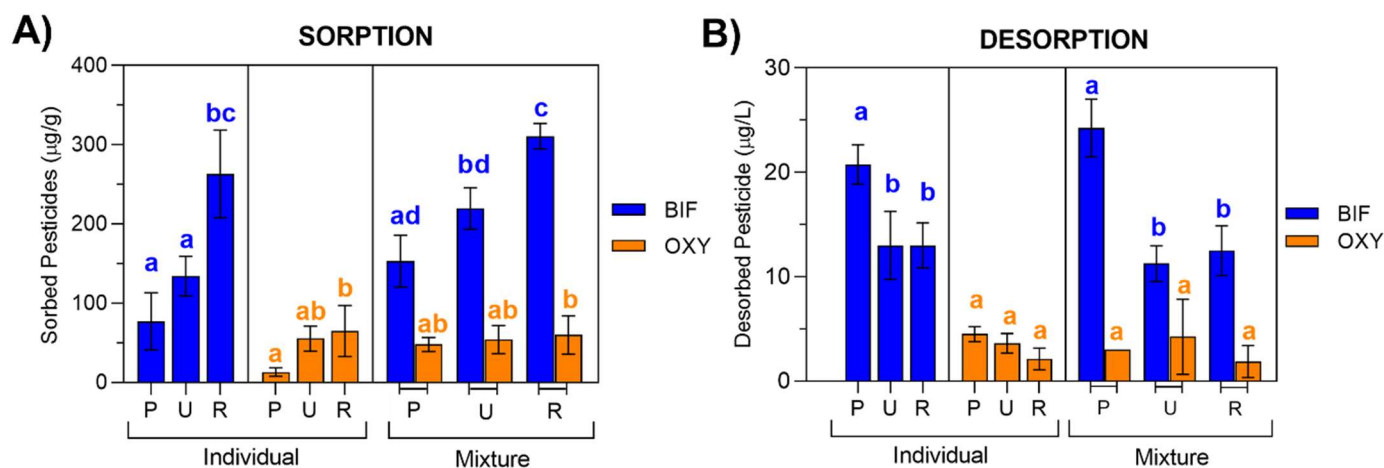


Figure 2. Sorption (A) and desorption (B) of BIF and OXY and BIF+OXY mixtures. Sorbed concentrations are expressed as μg of pesticide per unit mass of plastic ($\mu\text{g/g}$). Desorbed concentrations are expressed as μg of pesticide per unit volume of medium ($\mu\text{g/L}$). The results are expressed as mean \pm standard deviation ($n = 4$). Different letters indicated significant differences ($p < 0.05$; Tukey's HSD test).

and R. The desorption percentages presented in Fig. S3 (SM) were significantly higher in P with respect to U and R for both herbicides. Accordingly, BIF and OXY were preferentially retained in aged plastics consistent with the stronger sorption reported before. The negative correlation observed between sorption and desorption amounts (Table S4, SM) indicated that aged plastic tended to accumulate more herbicides than pristine fragments. Therefore, aged plastics have a higher capacity to behave as vectors for toxic chemicals.

3.3. Effect of individual and mixture herbicides leachates from P, U, and R pre-exposed plastics on the green alga *Chlamydomonas reinhardtii*

The results indicated that the exposure to leachates from control plastics (P, U and R non-exposed to herbicides) did not cause any significant effect on the total chlorophyll concentration in the green alga *C. reinhardtii* (Fig. 3 and Fig. S4, SM). On the contrary, leachates from plastics pre-exposed to the herbicides, significantly ($p < 0.05$) affected chlorophyll contents. The toxicity was clearly higher in leachates containing mixtures of the two herbicides. To discard an effect due to other chemicals that might be present in the herbicide leachates from the pre-exposed plastics, cells were also directly exposed to the same concentrations of BIF, OXY and the mixture BIF+OXY obtained in desorption experiments. The concentrations tested are shown in Table S5 (SM). In all cases the toxicity of desorbed herbicides was the same expected from the desorbed concentrations of herbicides according to the dose-response curves obtained for both compounds and their mixture and shown in Fig. S5 (SM). The results indicated that there was no evidence of other compounds causing toxic effects.

Toxicological interactions are an important issue when dealing with pollutant mixtures and their effects. The interactions between pollutants can be synergistic, or

antagonistic and depend on the extent of the impairment caused to a given organism. In this work, the Combination-Index (CI) method was applied based on the concentrations obtained in desorption experiments. First, the dose-response curves of BIF, OXY, and BIF+OXY were obtained as shown in Fig. S5A-E (SM). The ratio BIF:OXY used in mixtures was 20.4:2.5 in MIX-P, 9.3:3.5 in MIX-U and 11.0:1.7 in MIX-R according to the results obtained in desorption studies. The EC_{50} values for BIF, OXY and BIF+OXY mixtures are shown in Table S6 (SM). Because of their low EC_{50} , $29.5 \pm 1.9 \mu\text{g/L}$ and $4.0 \pm 0.6 \mu\text{g/L}$ for BIF and OXY respectively, both compounds can be considered toxic for microalgae ($EC_{50} < 1 \text{ mg/L}$) according to The EU Directive 93/67/EEC. Comparable microalgal toxicity data for these pesticides have been published elsewhere (Geoffroy et al., 2002; Jianyi et al., 2002).

The results from mixture experiments are shown as $CI-f_a$ plot in Fig. 4. CI values, calculated from Eq. 3, showed a clear antagonistic ($CI > 1$) interaction a low effect levels that turned synergistic ($CI < 1$) for higher chlorophyll content reduction. This tendency was observed for the mixtures desorbed from the three types of plastics meaning that the combined effect of BIF and OXY exceeded the toxicity of the individual components for $f_a > 0.2-0.4$. Antagonism at low effect levels followed by additivity or synergistic interaction at higher affected fractions was previously reported for different biological systems (Geoffroy et al., 2002; Almeida et al., 2017; Mansano et al., 2017). It is important to note that the CI index quantifies the type of interaction, but it is independent of the mechanisms of action of the pollutants. The mode of action of diphenyl ethers is similar. The members of this group interfere tetrapyrrole metabolism and inhibit the protoporphyrinogen oxidase, which gives rise to the accumulation of protoporphyrinogen in photosynthetically active cells. High levels of

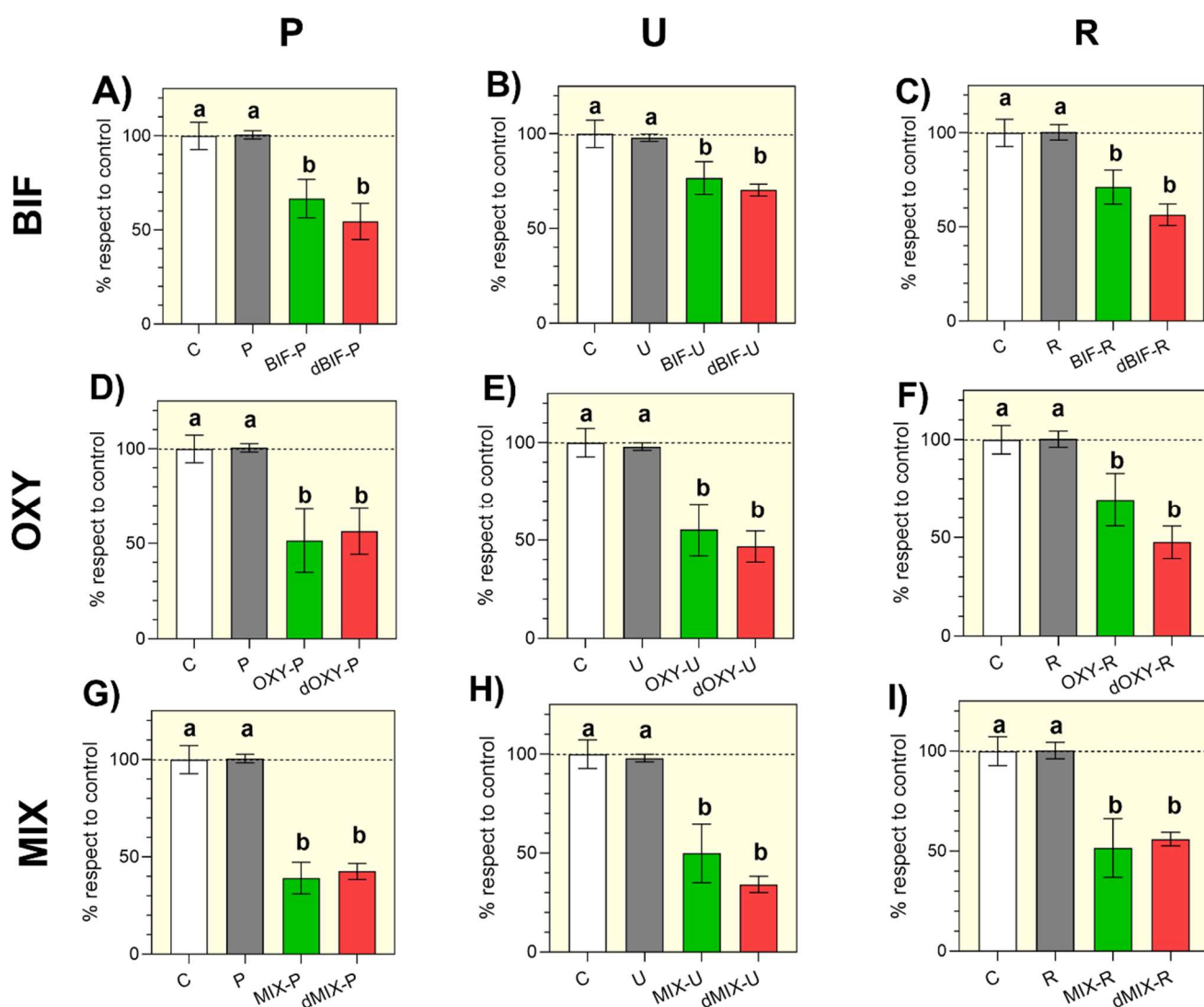


Figure 3. Total chlorophyll content of *C. reinhardtii* exposed to leachates of herbicides from P (A, D, G), U (B, E, H) and R (C, F, I). Cells were also exposed to the same concentrations of BIF, OXY and BIF+OXY measured in desorption experiments, which are denoted as dBIF-P/U/R, dOXY-P/U/R and dMIX-P/U/R (see Table S5, SM). Control “C” represents non-exposed cells. Results are expressed as percentage \pm SD with respect to control. Different letters indicate significant differences between treatments (Tukey’s HSD, $p < 0.05$).

tetrapyrroles enhance photosensitivity and lead to photooxidation. It was the aim of our study to test the hypothesis that similarly acting compounds could induce non-additive toxic responses as could be expected from their similar physicochemical characteristics. In this case, BIF and OXY have similar chemical structure and their mode of action are expected to be similar. However, their behavior departs from additivity. However, our results showed significant departures from additivity. The reason may be in the different toxicokinetic or toxicodynamic interactions that are taking place, like the different action of metabolizing enzymes. The molecular mechanisms underlying non-additive interactions in the combined exposure to several chemicals are very complex and can be due to a variety of reasons (Jia et al., 2009). It has been suggested that the antagonistic behavior observed in some cases at low affected fractions could be due to a competition for binding sites

that eventually reduced the activity of chemicals. It could be also explained by detoxification mechanisms acting at low herbicides doses (Geoffroy et al., 2002). The synergism found at higher levels of effect could be linked to differences in detoxification activities when cell have lost viability at high concentration of herbicides (Cedergreen, 2014).

Flow cytometry analyses to determine the toxicity mechanisms affecting *C. reinhardtii* after exposure to herbicides leachates were performed. The results, presented in Table S7 (SM) showed a decrease in cell size, complexity, and chlorophyll autofluorescence ($p < 0.05$) upon exposure. Changes in microalgal cell size and complexity exposed to different pollutants have been previously reported and attributed to the existence of chlorotic cells and growth inhibition responsible for decreased cell size and complexity (Seoane et al.,

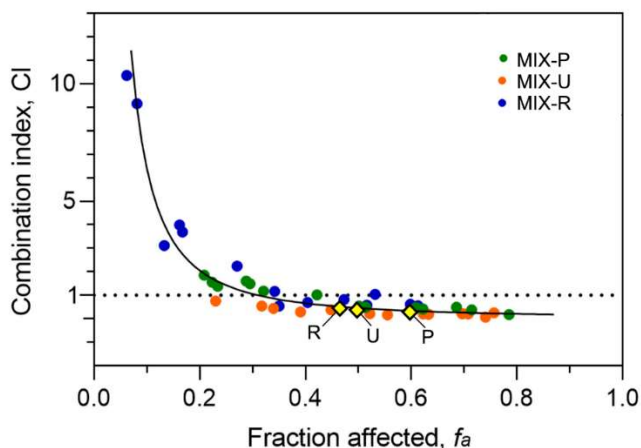


Figure 4. Combination index-fraction affected (CI- f_a) plot for dMIX-P, dMIX-U, and dMIX-R (Table S5). The fraction affected is the fractional inhibition of total chlorophyll content. CI < 1 indicates synergism; CI = 1 additivity and CI > 1 antagonism. Yellow diamonds represent the values corresponding to the concentrations in the leachates from pre-exposed P, U and R plastics.

2014). The decline in autofluorescence can be due to the loss of chlorophyll pigments (Fig. S4, SM) or damages in PSII photochemical activity, which is another common toxic response (Almeida et al., 2019).

No statistical differences were found between treatments (BIF, OXY, and MIX) (Table S7, SM).

The results obtained using different fluorochromes are presented in Fig. 5 and Figs. S6–S10 (SM). ROS overproduction is a usual finding when microalgae are subject to environmental stressors. Fig. 5A and Fig. S6 (SM), show that leachates containing BIF and OXY caused an increase of H_2O_2 levels ranging from 10 to 12% and 4–9% respectively, which were statistically significant for BIF with respect to non-exposed cells ($p < 0.05$). However, the mixture leachate, MIX, induced a significantly ROS decrease (between 6 and 18%), significant ($p < 0.05$) for MIX-R leachate. Regarding lipid peroxidation, a significant increase was observed in all treatments with respect to controls ($p < 0.05$) similar for BIF and OXY leachates and slightly higher for MIX leachates (Fig. 5B and Fig. S7, SM). The results for DiBAC₄(3) fluorescence indicated membrane hyperpolarization in all treatments (Fig. 5C and Fig. S8, SM). Likewise, a significant decrease in BCECF-AM green/red intensity ratio was observed ($p < 0.05$), revealing a decrease in intracellular pH (acidification) which was slightly higher for the mixture (Fig. 5D and Fig. S9, SM). The metabolic activity of microalgae cells (tracked by esterase activity using the fluorochrome FDA) indicated a significant ($p < 0.05$)

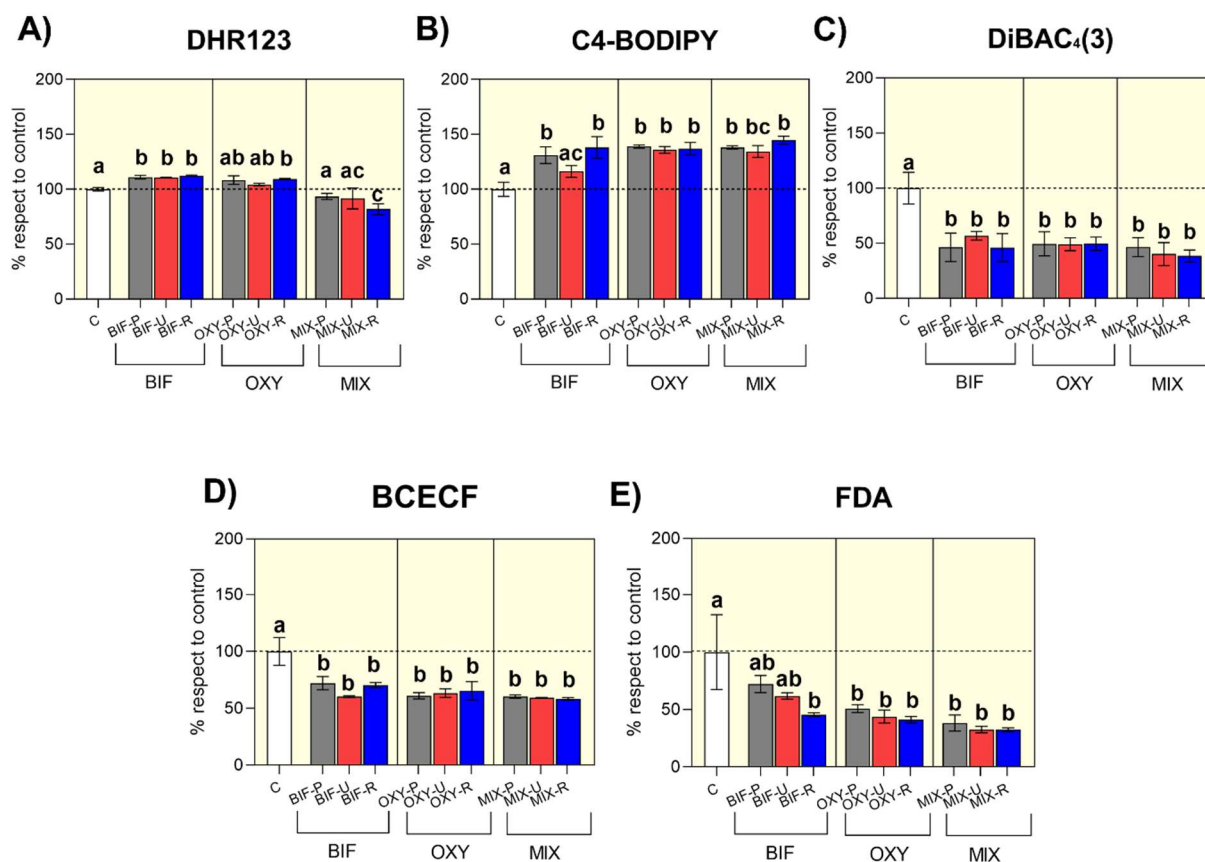


Figure 5. Flow cytometry results for *C. reinhardtii* after 72 h of exposure to herbicide leachates from P, U, and R pre-exposed plastics as measured by the indicated fluorochromes. A) ROS overproduction; B) lipid peroxidation (B); C) cytoplasmic membrane potential; D) intracellular pH; E) metabolic activity. Control (c) represents non-exposed microalgae cells. Results are expressed as percentage \pm SD with respect to control. Different letters indicate significant differences between treatments (Tukey's HSD, $p < 0.05$).

drop in all cases, especially in cells exposed to the mixture (Fig. 5E and Fig. S10 SM). As indicated before, the loss of photosynthetic pigments produced by the herbicides could induce ROS overproduction because of protoporphyrinogen IX accumulation (Kilinc et al., 2009). The lower ROS overproduction in cells exposed to the mixture leachate could be explained by the existence of chlorotic or dead cells, which agreed with the lower concentration of chlorophyll and could explain the observed synergistic interaction (Prado et al., 2012). The lipid peroxidation and changes in membrane potential might be a consequence of ROS overproduction. ROS overproduction could also explain the drop-in metabolic activity and the changes in intracellular pH observed as explained elsewhere (Seoane et al., 2017).

The toxicological effects observed on the microalgae tested in this work may have ecological relevance in view of the critical role played by these microorganisms in aquatic ecosystems. As an essential component of phytoplankton communities, any detrimental effect would affect oxygen and biomass production and carbon fixation in freshwater ecosystems. In addition, because microalgae are at the base of aquatic food chains, their impairment would propagate and affect higher levels of the freshwater trophic net (from zooplankton to fish) and, finally, the whole ecosystem and even the human health. Thus, in this new way, pesticides modulate their entry to freshwater ecosystems, making more likely the exposure of non-target organisms to different mixtures, this should be considered for ecological risk assessment.

4. Conclusions

The results showed that the aging of low-density polyethylene used for the manufacturing of agricultural pipes increased their capacity for the sorption and desorption of the two tested diphenyl-ether herbicides, bifenoX and oxyfluorfen. This was attributed to the higher polarity of aged plastics due to the presence of oxygenated moieties on their surface, and to their larger projected area, consequence of their numerous cracks and irregularities with respect to pristine materials.

Leachates from plastics pre-exposed to bifenoX, oxyfluorfen and their mixtures severely affected the green alga *Chlamydomonas reinhardtii*. The results showed overproduction of intracellular reactive oxygen species that triggered lipid peroxidation, hyperpolarization of cytoplasmic membrane potential, intracellular pH acidification, and metabolic impairment.

The use of Combination Index (CI)-isobologram method showed a clear departure from additivity in cells exposed to a mixture of both herbicides. Antagonism was clearly observed for low toxic effect levels, but the combination of herbicides, quickly tended to synergism as the affected fraction increased, meaning higher toxicity than expected considering additive behavior.

In real-exposure scenarios, plastics with different degrees of oxidation and surface alterations coexist with different chemicals, which can be sorbed and transported as the plastic moves through different compartments. The desorption of pollutant mixtures has the potential to seriously affect the biota. These facts need to be taken into account for the risk assessment of complex mixtures of plastics and chemicals.

Acknowledgments

The authors acknowledge the financial support provided by the Spanish Government (Ministerio de Ciencia e Innovación): PID2020-113769RBC21/22, PLEC2021-007693 and TED2021-131609B-C32/33, and the Thematic Network of Micro- and Nanoplastics in the Environment (RED2018-102345-T, EnviroPlaNet Network). IV thanks the Spanish Government for the award of a pre-doctoral FPI grant (BES-2017-080711).

References

- Almeida, A.C., Gomes, T., Langford, K., Thomas, K.V., Tollefsen, K.E., 2017. Oxidative stress in the algae *Chlamydomonas reinhardtii* exposed to biocides. *Aquatic Toxicology* 189, 50-59.
- Almeida, A.C., Gomes, T., Langford, K., Thomas, K.V., Tollefsen, K.E., 2019. Oxidative stress potential of the herbicides bifenoX and metribuzin in the microalgae *Chlamydomonas reinhardtii*. *Aquatic Toxicology* 210, 117-128.
- Bakir, A., Rowland, S.J., Thompson, R.C., 2012. Competitive sorption of persistent organic pollutants onto microplastics in the marine environment. *Marine Pollution Bulletin* 64, 2782-2789.
- Blunt, L., Jiang, X., 2003. Numerical parameters for characterisation of topography, in: *Advanced Techniques for Assessment Surface Topography: Development of a Basis for 3D Surface Texture Standards 'Surfstand'*. Kogan Page Science, Oxford, pp. 17-41.
- Brandon, J., Goldstein, M., Ohman, M.D., 2016. Long-term aging and degradation of microplastic particles: Comparing in situ oceanic and experimental weathering patterns. *Marine Pollution Bulletin* 110, 299-308.
- Cai, L., Wang, J., Peng, J., Wu, Z., Tan, X., 2018. Observation of the degradation of three types of plastic pellets exposed to UV irradiation in three different environments. *Science of The Total Environment* 628-629, 740-747.
- Carrasco, F., Pagès, P., Pascual, S., Colom, X., 2001. Artificial aging of high-density polyethylene by ultraviolet irradiation. *European Polymer Journal* 37, 1457-1464.
- Cedergreen, N., 2014. Quantifying Synergy: A systematic review of mixture toxicity studies within environmental toxicology. *PLOS ONE* 9, e96580.

- Chou T.C., 2010. Drug combination studies and their synergy quantification using the Chou-Talalay method. *Cancer Research* 70, 440-446.
- Chou, T.C., Martin, N., 2007. The mass-action law-based new computer software, CompuSyn, for automated simulation of synergism and antagonism in drug combination studies. *Cancer Research* 67, 637-637
- Comont, D., Lowe, C., Hull, R., Crook, L., Hicks, H.L., Onkokesung, N., Beffa, R., Childs, D.Z., Edwards, R., Freckleton, R.P., Neve, P., 2020. Evolution of generalist resistance to herbicide mixtures reveals a trade-off in resistance management. *Nature Communications* 11, 3086.
- Cusworth, S.J., Davies, W.J., McAinsh, M.R., Stevens, C.J., 2022. Sustainable production of healthy, affordable food in the UK: The pros and cons of plasticulture. *Food and Energy Security* 11, 4, e404.
- Edo, C., Fernández-Piñas, F., Rosal, R., 2022. Microplastics identification and quantification in the composted Organic Fraction of Municipal Solid Waste. *Science of The Total Environment* 813, 151902.
- EFSA, 2007. Conclusion on the peer review of bifenoxy. EFSA Scientific Report 119, pp. 1-84.
- Fajardo, C., Martín, C., Costa, G., Sánchez-Fortún, S., Rodríguez, C., de Lucas Burneo, J.J., Nande, M., Mengs, G., Martín, M., 2022. Assessing the role of polyethylene microplastics as a vector for organic pollutants in soil: Ecotoxicological and molecular approaches. *Chemosphere* 288, 132460.
- Feng, Q., An, C., Chen, Z., Yin, J., Zhang, B., Lee, K., Wang, Z., 2022. Investigation into the impact of aged microplastics on oil behavior in shoreline environments. *Journal of Hazardous Materials* 421, 126711.
- Geoffroy, L., Teisseire, H., Couderchet, M., Vernet, G., 2002. Effect of oxyfluorfen and diuron alone and in mixture on antioxidative enzymes of *Scenedesmus obliquus*. *Pesticide Biochemistry and Physiology* 72, 178-185.
- Gong, W., Jiang, M., Han, P., Liang, G., Zhang, T., Liu, G., 2019. Comparative analysis on the sorption kinetics and isotherms of fipronil on nondegradable and biodegradable microplastics. *Environmental Pollution* 254, 112927.
- González-Pleiter, M., Pedrouzo-Rodríguez, A., Verdú, I., Leganés, F., Marco, E., Rosal, R., Fernández-Piñas, F., 2021. Microplastics as vectors of the antibiotics azithromycin and clarithromycin: Effects towards freshwater microalgae. *Chemosphere* 268, 128824.
- Grossmann, K., 2005. What it takes to get a herbicide's mode of action. *Physionomics, a classical approach in a new complexion*. *Pest Management Science* 61, 423-431.
- Hartmann, N.B., Rist, S., Bodin, J., Jensen, L.H.S., Schmidt, S.N., Mayer, P., Meibom, A., Baun, A., 2017. Microplastics as vectors for environmental contaminants: Exploring sorption, desorption, and transfer to biota. *Integrated Environmental Assessment and Management* 13, 488-493.
- Ho, W.K., Leung, K.S.Y., 2019. Sorption and desorption of organic UV filters onto microplastics in single and multi-solute systems. *Environmental Pollution* 254, 113066.
- Ibrahim, A.M., Sayed, D.A., 2019. Toxicological impact of oxyfluorfen 24% herbicide on the reproductive system, antioxidant enzymes, and endocrine disruption of *Biomphalaria alexandrina* (Ehrenberg, 1831) snails. *Environmental Science and Pollution Research* 26, 7960-7968.
- Jeffrey, S. T., Humphrey, G.F. 1975. New spectrophotometric equations for determining chlorophylls a, b, c1 and c2 in higher plants, algae and natural phytoplankton. *Biochimie und Physiologie der Pflanzen*, 167, 2, 191-194.
- Jia, J., Zhu, F., Ma, X., Cao, Z.W., Li, Y.X., Chen, Y.Z., 2009. Mechanisms of drug combinations: interaction and network perspectives. *Nature Reviews Drug Discovery* 8, 111-128.
- Jiang, H., Wei, Y., Cheng, Q., Zhu, Z., 2018. Scratch behavior of low density polyethylene film: Effects of pre-stretch and aging. *Materials & Design* 157, 235-243.
- Jianyi, M., Ligen, X., Shufeng, W., 2002. A Quick, Simple, and accurate method of screening herbicide activity using green algae cell suspension cultures. *Weed Science* 50, 555-559.
- Kilinc, Ö., Reynaud, S., Perez, L., Tissut, M., Ravanel, P., 2009. Physiological and biochemical modes of action of the diphenylether acetonif. *Pesticide Biochemistry and Physiology* 93, 65-71.
- Lan, T., Wang, T., Cao, F., Yu, C., Chu, Q., Wang, F., 2021. A comparative study on the adsorption behavior of pesticides by pristine and aged microplastics from agricultural polyethylene soil films. *Ecotoxicology and Environmental Safety* 209, 111781.
- Lin, J., Wu, X., Liu, Y., Fu, J., Chen, Y., Ou, H., 2022. Sinking behavior of polystyrene microplastics after disinfection. *Chemical Engineering Journal* 427, 130908.
- Liu, G., Zhu, Z., Yang, Y., Sun, Y., Yu, F., Ma, J., 2019. Sorption behavior and mechanism of hydrophilic organic chemicals to virgin and aged microplastics in freshwater and seawater. *Environmental Pollution* 246, 26-33.
- Lundqvist, J., von Brömssen, C., Rosenmai, A.K., Ohlsson, Å., Le Godec, T., Jonsson, O., Kreuger, J., Oskarsson, A., 2019. Assessment of pesticides in surface water samples from Swedish agricultural areas by integrated bioanalysis and chemical analysis. *Environmental Sciences Europe* 31, 53.
- Mansano, A.S., Moreira, R.A., Dornfeld, H.C., Freitas, E.C., Vieira, E.M., Sarmento, H., Rocha, O., Selegim, M.H.R., 2017. Effects of diuron and carbofuran and their mixtures on the microalgae

- Raphidocelis subcapitata*. Ecotoxicology and Environmental Safety 142, 312-321.
- McHale, G., Newton, M.I., Shirtcliffe, N.J., 2005. Water-repellent soil and its relationship to granularity, surface roughness and hydrophobicity: a materials science view. European Journal of Soil Science 56, 445-452.
- Nerín, C., Tornés, A.R., Domeño, C., Cacho, J., 1996. Absorption of Pesticides on Plastic Films Used as Agricultural Soil Covers. Journal of Agricultural and Food Chemistry 44, 4009-4014.
- Nizzetto, L., Langaas, S., Futter, M., 2016. Pollution: Do microplastics spill on to farm soils? Nature 537, 488-488.
- Peris, A., Barbieri, M.V., Postigo, C., Rambla-Alegre, M., López de Alda, M., Eljarrat, E., 2022. Pesticides in sediments of the Ebro River Delta cultivated area (NE Spain): Occurrence and risk assessment for aquatic organisms. Environmental Pollution 305, 119239.
- Piehl, S., Leibner, A., Löder, M.G.J., Dris, R., Bogner, C., Laforsch, C., 2018. Identification and quantification of macro- and microplastics on an agricultural farmland. Scientific Reports 8, 17950.
- Pinal, R., Rao, P.S.C., Lee, L.S., Cline, P.V., Yalkowsky, S.H. Cosolvency of partially miscible organic solvents on the solubility of hydrophobic organic chemicals. Environ. Sci. Technol., 24 (5) (1990), pp. 639-647.
- Prado, R., Rioboo, C., Herrero, C., Suárez-Bregua, P., Cid, Á., 2012. Flow cytometric analysis to evaluate physiological alterations in herbicide-exposed *Chlamydomonas moewusii* cells. Ecotoxicology 21, 409-420.
- Rehm, R., Zeyer, T., Schmidt, A., Fiener, P., 2021. Soil erosion as transport pathway of microplastic from agriculture soils to aquatic ecosystems. Science of The Total Environment 795, 148774.
- Székács, A. Herbicide mode of action, in: Robin Mesnage and Johann G. Zaller (Eds.) Emerging Issues in Analytical Chemistry - Herbicides: Chemistry, Efficacy, Toxicology, and Environmental Impacts, pp. 41-86, Elsevier, 2021.
- Seoane, M., Rioboo, C., Herrero, C., Cid, Á., 2014. Toxicity induced by three antibiotics commonly used in aquaculture on the marine microalga *Tetraselmis suecica* (Kyllin) Butch. Marine Environmental Research 101, 1-7.
- Seoane, M., Esperanza, M., Cid, Á., 2017. Cytotoxic effects of the proton pump inhibitor omeprazole on the non-target marine microalga *Tetraselmis suecica*. Aquatic Toxicology, 191, 62-72.
- Sorasan, C., Edo, C., González-Pleiter, M., Fernández-Piñas, F., Leganés, F., Rodríguez, A., Rosal, R., 2021. Generation of nanoplastics during the photoageing of low-density polyethylene. Environmental Pollution 289, 117919.
- Sorasan, C., Edo, C., González-Pleiter, M., Fernández-Piñas, F., Leganés, F., Rodríguez, A., Rosal, R., 2022. Ageing and fragmentation of marine microplastics, Science of The Total Environment 827, 154438.
- ter Halle, A., Ladirat, L., Martignac, M., Mingotaud, A.F., Boyron, O., Perez, E., 2017. To what extent are microplastics from the open ocean weathered? Environmental Pollution 227, 167-174.
- Verdú, I., González-Pleiter, M., Leganés, F., Rosal, R., Fernández-Piñas, F., 2021. Microplastics can act as vector of the biocide triclosan exerting damage to freshwater microalgae. Chemosphere 266, 129193.
- Wang, T., Yu, C., Chu, Q., Wang, F., Lan, T., Wang, J., 2020. Adsorption behavior and mechanism of five pesticides on microplastics from agricultural polyethylene films. Chemosphere 244, 125491.
- Wu, X., Liu, P., Huang, H., Gao, S., 2020. Adsorption of triclosan onto different aged polypropylene microplastics: Critical effect of cations. Science of The Total Environment 717, 137033.
- You, H., Huang, B., Cao, C., Liu, X., Sun, X., Xiao, L., Qiu, J., Luo, Y., Qian, Q., Chen, Q., 2021. Adsorption-desorption behavior of methylene blue onto aged polyethylene microplastics in aqueous environments. Marine Pollution Bulletin 167, 112287.
- Zhang, C., Lei, Y., Qian, J., Qiao, Y., Liu, J., Li, S., Dai, L., Sun, K., Guo, H., Sui, G., Jing, W., 2021. Sorption of organochlorine pesticides on polyethylene microplastics in soil suspension. Ecotoxicology and Environmental Safety 223, 112591.
- Zhou, B., Wang, J., Zhang, H., Shi, H., Fei, Y., Huang, S., Tong, Y., Wen, D., Luo, Y., Barceló, D., 2020. Microplastics in agricultural soils on the coastal plain of Hangzhou Bay, east China: Multiple sources other than plastic mulching film. Journal of Hazardous Materials 388, 121814.
- Zvekcic, M., Richards, L.C., Tong, C.C., Krogh, E.T., 2022. Characterizing photochemical ageing processes of microplastic materials using multivariate analysis of infrared spectra. Environmental Science: Processes & Impacts 24, 52-61.

Supplementary Material

Leaching of herbicides mixtures from pre-exposed agricultural plastics severely impact microalgae

Irene Verdú¹, Miguel González-Pleiter¹, Francisco Leganés^{1,2}, Francisca Fernández-Piñas^{1,2}, Roberto Rosal^{3,*}

¹ Department of Biology, Faculty of Science, Universidad Autónoma de Madrid, E-28049, Madrid, Spain

² Department of Chemical Engineering, Universidad de Alcalá, E-28871, Alcalá de Henares, Madrid, Spain

³ Centro de Investigación en Biodiversidad y Cambio Global (CIBC-UAM), Universidad Autónoma de Madrid, Darwin 2, 28049, Madrid, Spain

Contents:

Table S1. Physicochemical properties of bifenox (BIF) and oxyfluorfen (OXY).

Table S2. Fluorochromes used to analyze the physiological parameters of *C. reinhardtii* by flow cytometry.

Table S3. Hydroxyl and carbonyl indexes from the plastics used in this work.

Table S4. Spearman's correlation coefficients between sorption and desorption of pesticides ($\mu\text{g/g}$) and PE-MP characteristics. The asterisks represent a significant correlation between variables.

Table S5. Concentrations of herbicides, bifenox (BIF), and oxyfluorfen (OXY) measured in leachates from the pre-exposure of plastics P, U, and R and final concentrations resulting in the leachates tested in bioassays. (Tested concentrations represented 8.5 % of the initially measured in leachates due to the dilution with microalgal cells and culture medium.)

Table S6. Dose-response parameters for total chlorophyll concentration at 72 h, after individual exposure to BIF ($\mu\text{g/L}$), OXY ($\mu\text{g/L}$), and their mixtures at ratios determined by the desorbed concentrations from each plastic.

Table S7. Cell size, cell complexity, and cell autofluorescence of microalgae exposed to the leachates of the indicated treatments. Results are present as mean of fluorescence intensity (a.u) \pm SD ($n = 3$, $n = 6$ in control). The different letters indicated significant differences between treatments ($p < 0.05$) by Tukey's HSD test.

Figure S1. Agricultural plastics collected at different stages of environmental aging. Pristine plastics (P) were acquired new from a local retailer, plastic in use from a farmland (U), and plastics improperly discarded in a nearby riverbed (R). Images were taken prior to washing with distilled water and cutting (2 x 1.8 mm fragments).

Figure. S2. Schematic diagram of the experimental set-up.

Figure S3. Percentages of sorption (A) of BIF, OXY, and their mixture onto plastics P, U, and R, and percentages of desorption (B) of herbicides in leachates from the pre-exposed plastics to herbicides. The results are expressed as mean \pm SD ($n = 4$). The different letters indicated significant differences between treatments (Tukey's HSD, $p < 0.05$). Statistical tests were applied by type of pesticide and compared between different plastic and individual and mixture exposure of plastic to the herbicides.

Figure S4. Effect of the leachates from the pre-exposure of agricultural plastics to BIF (BIF-P, BIF-U, and BIF-R), OXY (OXY-P, OXY-U, and OXY-R) on total chlorophyll content of *Chlamydomonas reinhardtii* after 72 h of exposure. Control (C) represents non-exposed cells. Results are expressed as percentage \pm SD with respect to control (100% is indicated by the dashed line). Different letters indicate significant differences between treatments (Tukey's HSD, $p < 0.05$).

Figure S5. Dose-response curves of the effect of BIF (A) OXY (B), and their mixture (BIF+OXY) (C, D, E). The dose-response curves in mixtures were performed at a fixed ratio according to measured desorbed concentrations from the herbicide mixture pre-exposure to plastics P, U, and R. The BIF:OXY ratios were

20.4:2.5 (C), 9.3:3.5 (D), and 11.0:1.7 (F). In each graph, the diamonds indicate the desorbed concentrations of BIF, OXY, and their mixture released from their pre-exposures with P, U, and R, at which *C. reinhardtii* was exposed in bioassays.

Figure S6. Representative dot plot of the DHR123 fluorescence in a logarithmic scale, showing the effect on ROS (H_2O_2) production of *C. reinhardtii* of the leachates released from pre-exposure pristine (P) agricultural plastics to BIF (B), OXY (E), and MIX (BIF+OXY) (H); agricultural plastics in use from farmland (U) to BIF (C), OXY (F) and MIX (I); and agricultural plastics abandoned in a riverbed to BIF (D), OXY (G), and MIX (BIF+OXY) (J). The exposure time of the leachates to the organism was 72 h. (A) represents the ROS (H_2O_2) production in control cells (untreated cells). Y-axis represents fluorescence intensity in arbitrary units and X-axis the fluorescence intensity in arbitrary units. Values are shown as mean \pm SD of the percentage of DHR123+ cells (n = 3, n = 6 control).

Figure S7. Representative dot plot of the C4C9-BODIPY® fluorescence in a logarithmic scale, showing the effect on lipid peroxidation of *C. reinhardtii* of the leachates released from pre-exposure of pristine (P) agricultural plastics to BIF (B), OXY (E), and MIX (BIF+OXY) (H); agricultural plastics in use from farmland (U) to BIF (C), OXY (F) and MIX (I); and agricultural plastics abandoned in a riverbed to BIF (D), OXY (G), and MIX (BIF+OXY) (J). The exposure time of the leachates to the organism was 72 h. (A) represents the ROS (H_2O_2) production in control cells (untreated cells). Y-axis represents fluorescence intensity in arbitrary units and X-axis the fluorescence intensity in arbitrary units. Values are shown as mean \pm SD of the percentage of DHR123+ cells (n = 3, n = 6 control).

Figure S8. Representative histograms of the DiBAC₄(3) fluorescence in a logarithmic scale, showing the effect on the membrane potential of *C. reinhardtii* of the leachates released from pre-exposure of pristine (P) agricultural plastics to BIF (B), OXY (E), and MIX (BIF+OXY) (H); agricultural plastics in use from farmland (U) to BIF (C), OXY (F) and MIX (I); and agricultural plastics abandoned in a riverbed to BIF (D), OXY (G), and MIX (BIF+OXY) (J). The exposure time of the leachates to the organism was 72 h. (A) represents the ROS (H_2O_2) production in control cells (untreated cells). Y-axis represents fluorescence intensity in arbitrary units and X-axis the fluorescence intensity in arbitrary units. Values are shown as mean \pm SD of the percentage of DHR123+ cells (n = 3, n = 6 control).

Figure S9. Representative dot plot of the BCECF fluorescence in a logarithmic scale, showing the effect to intracellular pH of *C. reinhardtii* of the leachates released from pre-exposure of pristine (P) agricultural plastics to BIF (B), OXY (E), and MIX (BIF+OXY) (H); agricultural plastics in use from farmland (U) to BIF (C), OXY (F) and MIX (I); and agricultural plastics abandoned in a riverbed to BIF (D), OXY (G), and MIX (BIF+OXY) (J). The exposure time of the leachates to the organism was 72 h. (A) represents the ROS (H_2O_2) production in control cells (untreated cells). Y-axis represents fluorescence intensity in arbitrary units and X-axis the fluorescence intensity in arbitrary units. Values are shown as mean \pm SD of the percentage of DHR123+ cells (n = 3, n = 6 control).

Figure S10. Representative histograms of the distribution of FDA fluorescence in a logarithmic scale, showing the effect on the metabolic activity of *C. reinhardtii* of the leachates released from pre-exposure of pristine (P) agricultural plastics to BIF (B), OXY (E), and MIX (BIF+OXY) (H); agricultural plastics in use from farmland (U) to BIF (C), OXY (F) and MIX (I); and agricultural plastics abandoned in a riverbed to BIF (D), OXY (G), and MIX (BIF+OXY) (J). The exposure time of the leachates to the organism was 72 h. (A) represents the ROS (H_2O_2) production in control cells (untreated cells). Y-axis represents fluorescence intensity in arbitrary units and X-axis the fluorescence intensity in arbitrary units. Values are shown as mean \pm SD of the percentage of DHR123+ cells (n = 3, n = 6 control).

Table S1. Physicochemical properties of bifenoxy (BIF) and oxyfluorfen (OXY).

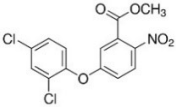
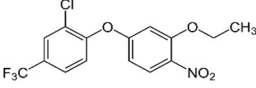
Herbicides	Molecular Formula	Molecular weight (g/mol)	Chemical structure	Log K _{ow}	Water Solubility (mg/L) (25 °C)
Bifenoxy (BIF)	C ₁₄ H ₉ Cl ₂ NO ₅	342.13		4.48	~0.5
Oxyfluorfen (OXY)	C ₁₅ H ₁₁ ClF ₃ NO ₄	361.70		4.73	~0.1

Table S2. Fluorochromes used to analyze the physiological parameters of *C. reinhardtii* by flow cytometry.

Fluorochrome	Acronym	Application	Stock concentration	Final concentration	Incubation Time (min)
fluorescein diacetate	FDA	Metabolic activity	5000 µg/mL	2.5 µg/mL	15
dihydrorhodamine 123	DHR123	Intracellular reactive oxygen species (hydrogen peroxide)	2000 µg/mL	10 µg/mL	40
bis-(1,3-dibutylbarbituric acid) trimethine oxonol	DiBAC ₄ (3)	cytoplasmic membrane potential	500 µg/mL	2.5 µg/mL	10
C4, C9-BODIPY®.	BODYPI	Level of cellular lipid peroxidation	1000 µg/mL	10 µg/mL	10
20,70-bis(2-carboxyethyl)-5(6)-carboxyfluorescein	BCECF-AM	Intracellular pH	1000 µg/mL	5 µg/mL	40

Table S3. Hydroxyl and carbonyl indexes from the plastics used in this work.

	Hydroxyl index	Carbonyl index
Pristine (P)	0.063 ± 0.014	1.27 ± 0.66
In Use (U)	0.176 ± 0.055	2.99 ± 0.53
In River (R)	0.191 ± 0.097	3.33 ± 0.85

Table S4. Spearman's correlation coefficients between sorption and desorption of pesticides (µg/g) and PE-MP characteristics. The asterisks represent a significant correlation between variables.

	Sorption		Desorption	
	BIF	OXY	BIF	OXY
Hydroxyl index	0.584*	0.425*	-0.642*	-0.401*
Carbonyl index	0.403*	0.607*	-0.695*	-0.360
% Crystallinity	-0.410*	-0.069*	-0.056	-0.102
T _g	-0.126	-0.066	0.249	0.256
T _m	0.041	-0.210	0.487*	0.319
Texture (<i>Sdr</i>)	0.599*	0.494*	-0.788*	-0.278
Texture (<i>Sku</i>)	0.485*	0.019	-0.292	-0.098
Hydrophobicity	0.840*	0.498*	-0.637*	-0.398
Presence of Cosolvent	0.473*	0.362	0.223	-0.146
Sorption	-	-	-0.498*	-0.619*

Table S5. Concentrations of herbicides, bifenox (BIF), and oxyfluorfen (OXY) measured in leachates from the pre-exposure of plastics P, U, and R and final concentrations resulting in the leachates tested in bioassays. (Tested concentrations represented 8.5 % of the initially measured in leachates due to the dilution with microalgal cells and culture medium.)

Treatment	Herbicide concentration measured in leachates ($\mu\text{g/L}$)		Herbicide concentration in leachates tested in bioassays ($\mu\text{g/L}$)	
	BIF	OXY	BIF	OXY
BIF-P	21	-	17.8	-
BIF-U	13	-	11.0	-
BIF-R	13	-	11.0	-
OXY-P	-	4.5	-	3.8
OXY-U	-	3.6	-	3.0
OXY-R	-	2.1	-	1.8
MIX-P	24	3	20.4	2.5
MIX-U	11	4	9.3	3.4
MIX-R	17	2	11.0	1.7

Not detected (-)

Table S6. Dose-response parameters for total chlorophyll concentration at 72 h, after individual exposure to BIF ($\mu\text{g/L}$), OXY ($\mu\text{g/L}$), and their mixtures at ratios determined by the desorbed concentrations from each plastic.

Compound	Ratio (BIF: OXY; $\mu\text{g/L}$)	EC ₅₀	SD	95 % Confidence Interval	r ²
BIF	-	29.5	1.9	18.7-40.3	0.96
OXY	-	4.0	0.6	2.68-5.21	0.96
MIX (BIF+OXY)	20.4: 2.55 (P)	13.6	0.9	11.7-15.4	0.99
	9.35: 3.4 (U)	3.2	0.4	2.32-4.08	0.98
	10.6: 1.7 (R)	13.9	3.1	7.28-20.5	0.86

Table S7. Cell size, cell complexity, and cell autofluorescence of microalgae exposed to the leachates of the indicated treatments. Results are present as mean of fluorescence intensity (a.u) \pm SD (n = 3, n = 6 in control). The different letters indicated significant differences between treatments ($p < 0.05$) by Tukey's HSD test.

	Treatment	Cell size (FSC-A, a.u.)	Cell complexity (SSC-A, a.u.)	Autofluorescence Chl. (APC, a.u.)
	Control	10955 \pm 166.2a	69889 \pm 6226a	67222 \pm 1087a
BIF	BIF-P	9225 \pm 211.5b	45557 \pm 5527b	42821 \pm 1651b
	BIF-U	9451 \pm 65.58b	44354 \pm 5828b	43398 \pm 1350b
	BIF-R	8984 \pm 92.37b	39143 \pm 2729b	39513 \pm 636.5b
OXY	OXY-P	9000 \pm 414.1b	40896 \pm 816.7b	39931 \pm 1798b
	OXY-U	9228 \pm 18.53b	37345 \pm 576.9b	40496 \pm 779.6b
	OXY-R	9868 \pm 18.53b	37270 \pm 1558b	44757 \pm 4319b
MIX	MIX-P	9096 \pm 120.1b	38705 \pm 622.5b	42533 \pm 1303b
	MIX-U	8985 \pm 114.1b	35241 \pm 672.1b	41021 \pm 772.1b
	MIX-R	9103 \pm 26.73b	35553 \pm 694.3b	41805 \pm 1364b

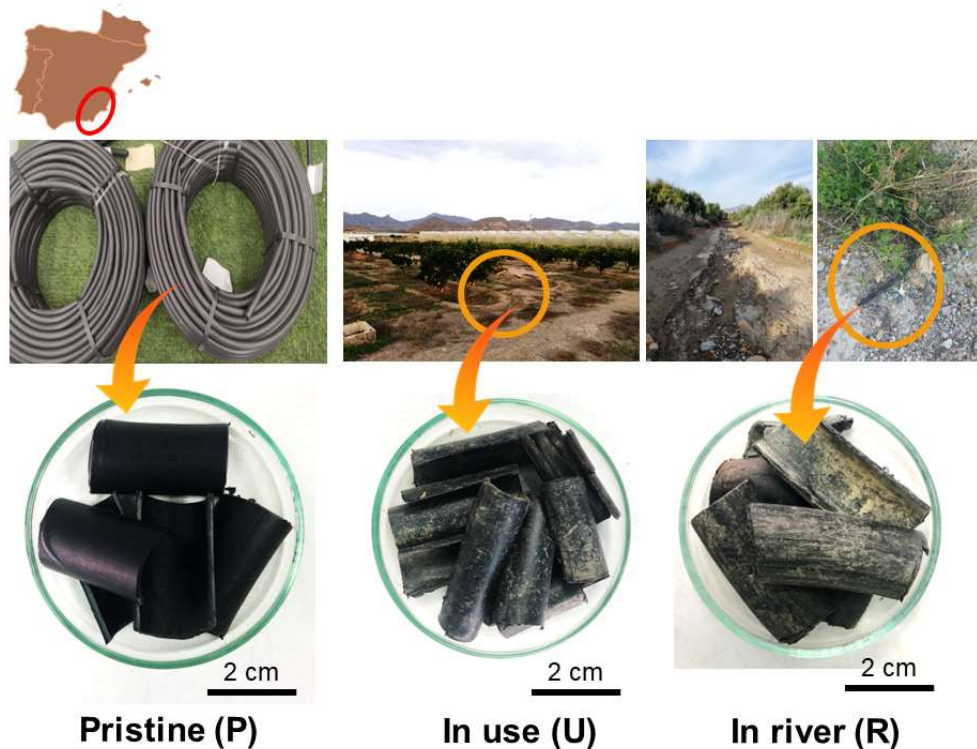


Figure S1. Agricultural plastics collected at different stages of environmental aging. Pristine plastics (P) were acquired new from a local retailer, plastic in use from a farmland (U), and plastics improperly discarded in a nearby riverbed (R). Images were taken prior to washing with distilled water and cutting (2 x 1.8 mm fragments).

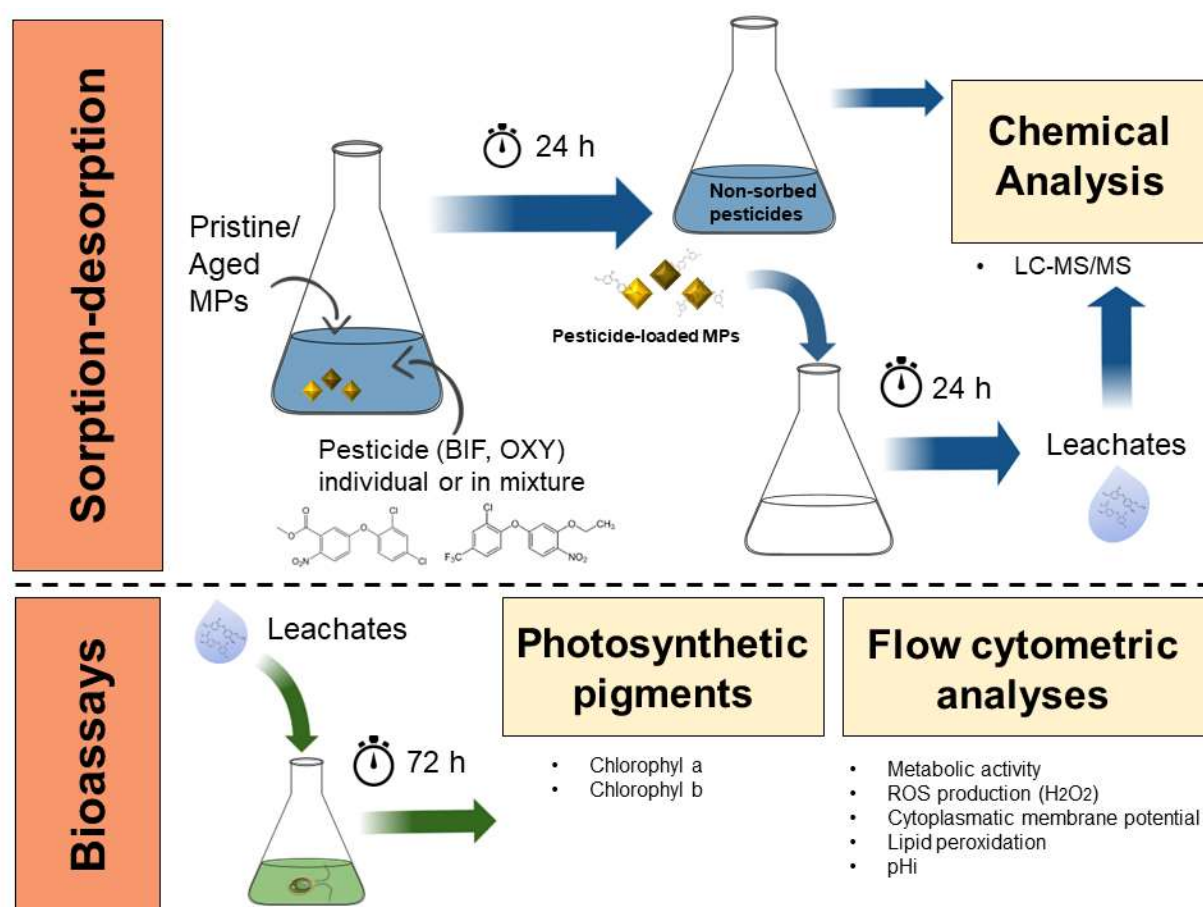


Figure. S2. Schematic diagram of the experimental set-up.

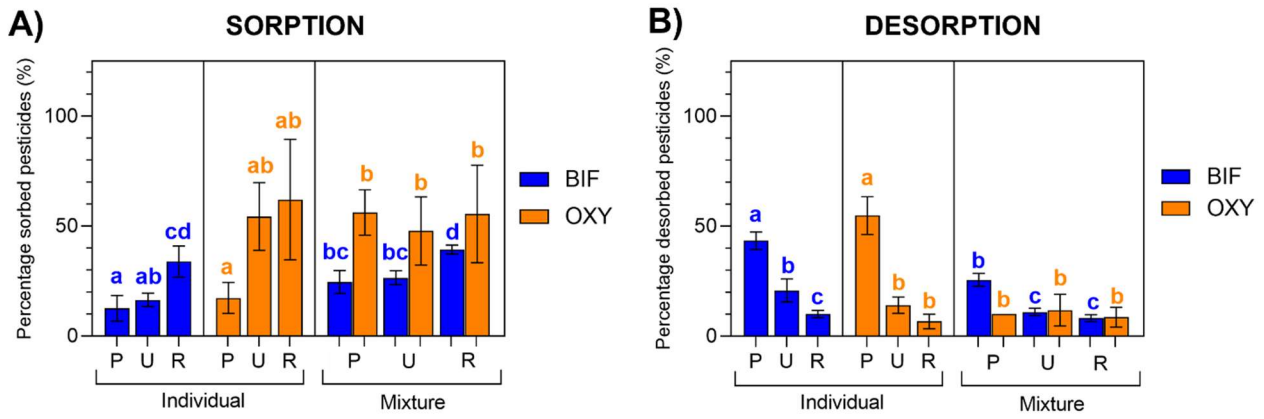


Figure S3. Percentages of sorption (A) of BIF, OXY, and their mixture onto plastics P, U, and R, and percentages of desorption (B) of herbicides in leachates from the pre-exposed plastics to herbicides. The results are expressed as mean \pm SD ($n = 4$). The different letters indicated significant differences between treatments (Tukey's HSD, $p < 0.05$). Statistical tests were applied by type of pesticide and compared between different plastic and individual and mixture exposure of plastic to the herbicides.

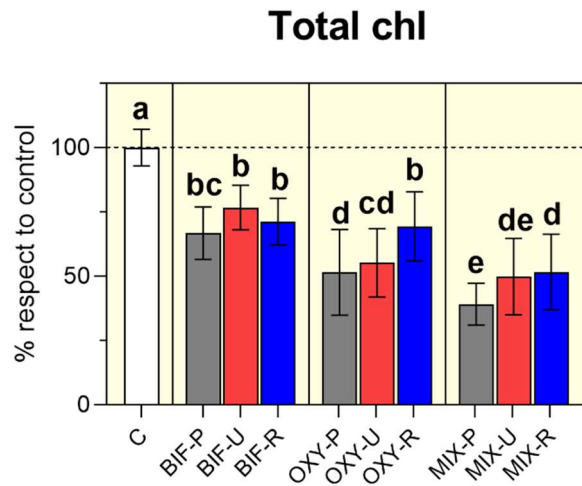


Figure S4. Effect of the leachates from the pre-exposure of agricultural plastics to BIF (BIF-P, BIF-U, and BIF-R), OXY (OXY-P, OXY-U, and OXY-R) on total chlorophyll content of *Chlamydomonas reinhardtii* after 72 h of exposure. Control (c) represents non-exposed cells. Results are expressed as percentage \pm SD with respect to control (100% is indicated by the dashed line). Different letters indicate significant differences between treatments (Tukey's HSD, $p < 0.05$).

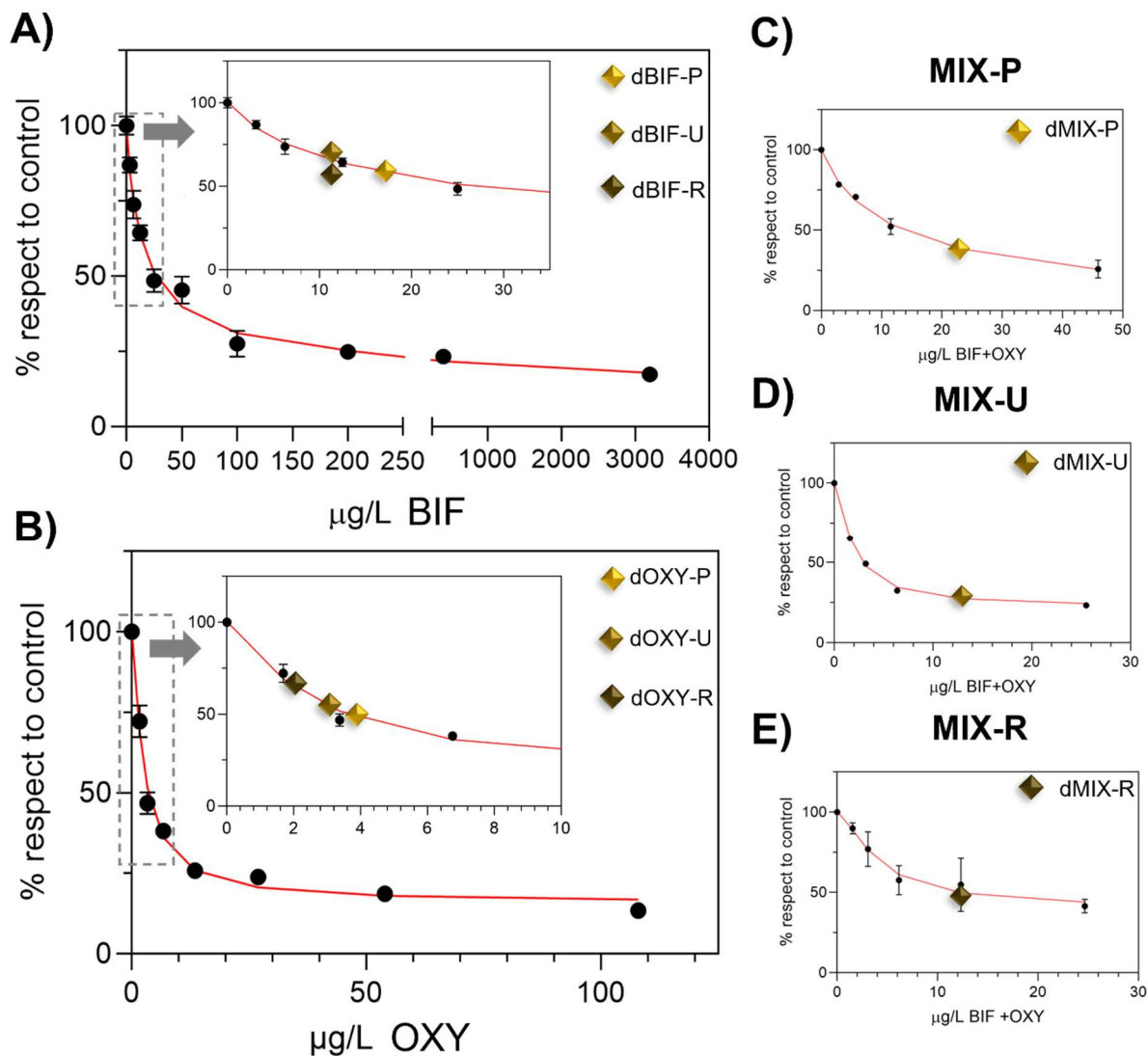


Figure S5. Dose-response curves of the effect of BIF (A) OXY (B), and their mixture (BIF+OXY) (C, D, E). The dose-response curves in mixtures were performed at a fixed ratio according to measured desorbed concentrations from the herbicide mixture pre-exposure to plastics P, U, and R. The BIF:OXY ratios were 20.4:2.5 (C), 9.3:3.5 (D), and 11.0:1.7 (F). In each graph, the diamonds indicate the desorbed concentrations of BIF, OXY, and their mixture released from their pre-exposures with P, U, and R, at which *C. reinhardtii* was exposed in bioassays.

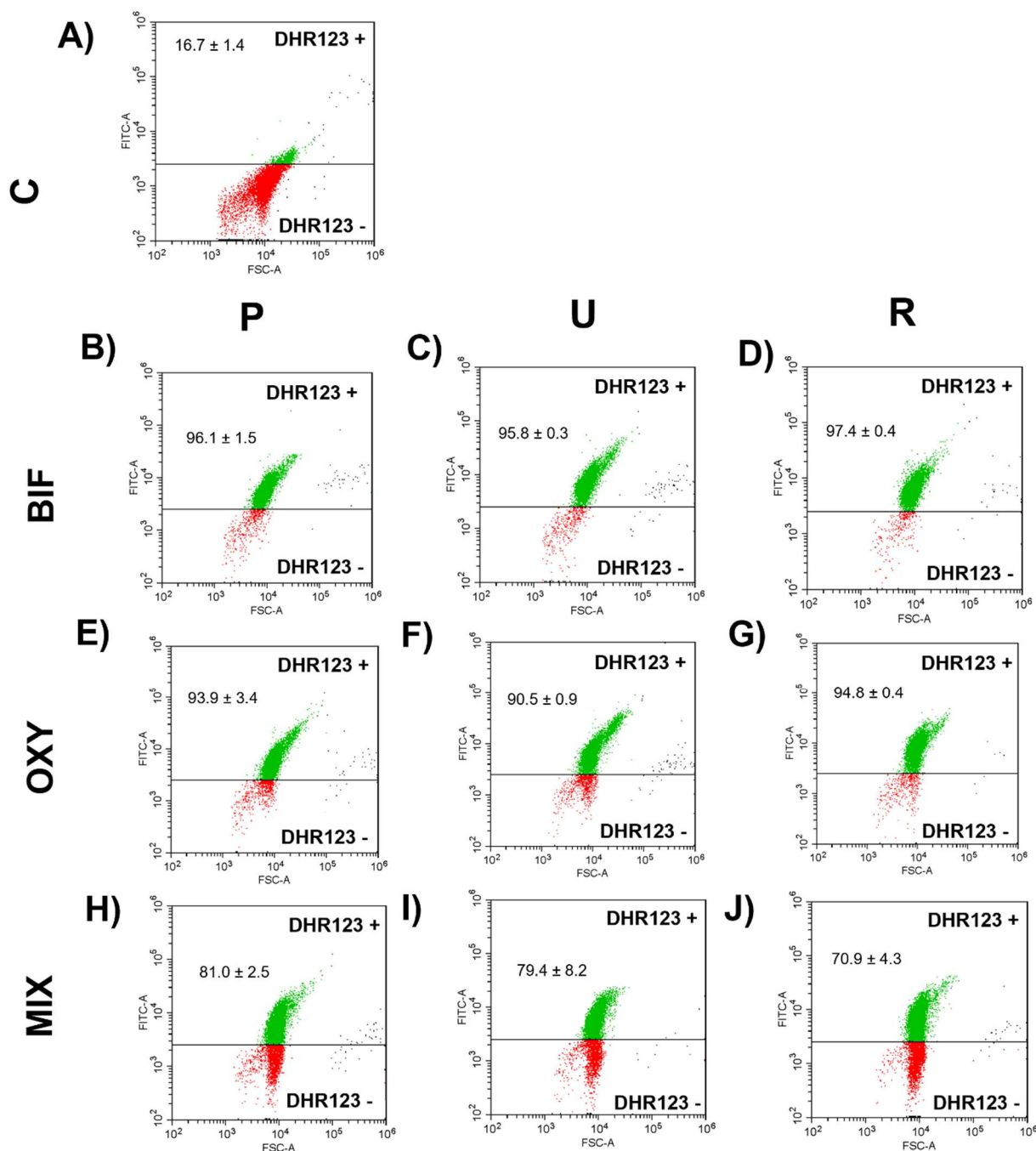


Figure S6. Representative dot plot of the DHR123 fluorescence in a logarithmic scale, showing the effect on ROS (H_2O_2) production of *C. reinhardtii* of the leachates released from pre-exposure pristine (P) agricultural plastics to BIF (B), OXY (E), and MIX (BIF+OXY) (H); agricultural plastics in use from farmland (U) to BIF (C), OXY (F) and MIX (I); and agricultural plastics abandoned in a riverbed to BIF (D), OXY (G), and MIX (BIF+OXY) (J). The exposure time of the leachates to the organism was 72 h. (A) represents the ROS (H_2O_2) production in control cells (untreated cells). Y-axis represents fluorescence intensity in arbitrary units and X-axis the fluorescence intensity in arbitrary units. Values are shown as mean \pm SD of the percentage of DHR123+ cells ($n = 3$, $n = 6$ control).

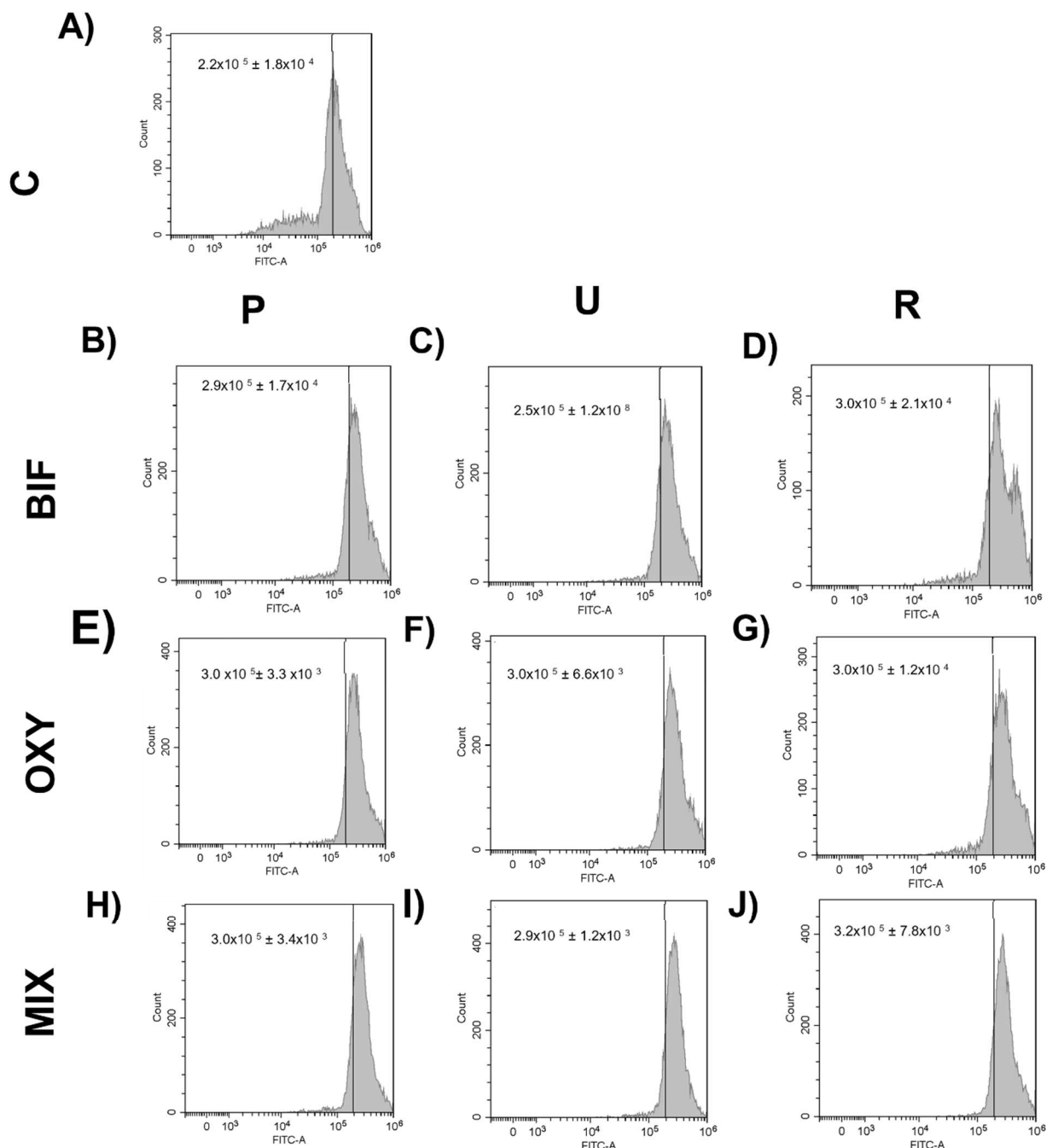


Figure S7. Representative dot plot of the C4C9-BODIPY® fluorescence in a logarithmic scale, showing the effect on lipid peroxidation of *C. reinhardtii* of the leachates released from pre-exposure of pristine (P) agricultural plastics to BIF (B), OXY (E), and MIX (BIF+OXY) (H); agricultural plastics in use from farmland (U) to BIF (C), OXY (F) and MIX (I); and agricultural plastics abandoned in a riverbed to BIF (D), OXY (G), and MIX (BIF+OXY) (J). The exposure time of the leachates to the organism was 72 h. (A) represents the ROS (H₂O₂) production in control cells (untreated cells). Y-axis represents fluorescence intensity in arbitrary units and X-axis the fluorescence intensity in arbitrary units. Values are shown as mean \pm SD of the percentage of DHR123+ cells (n = 3, n = 6 control).

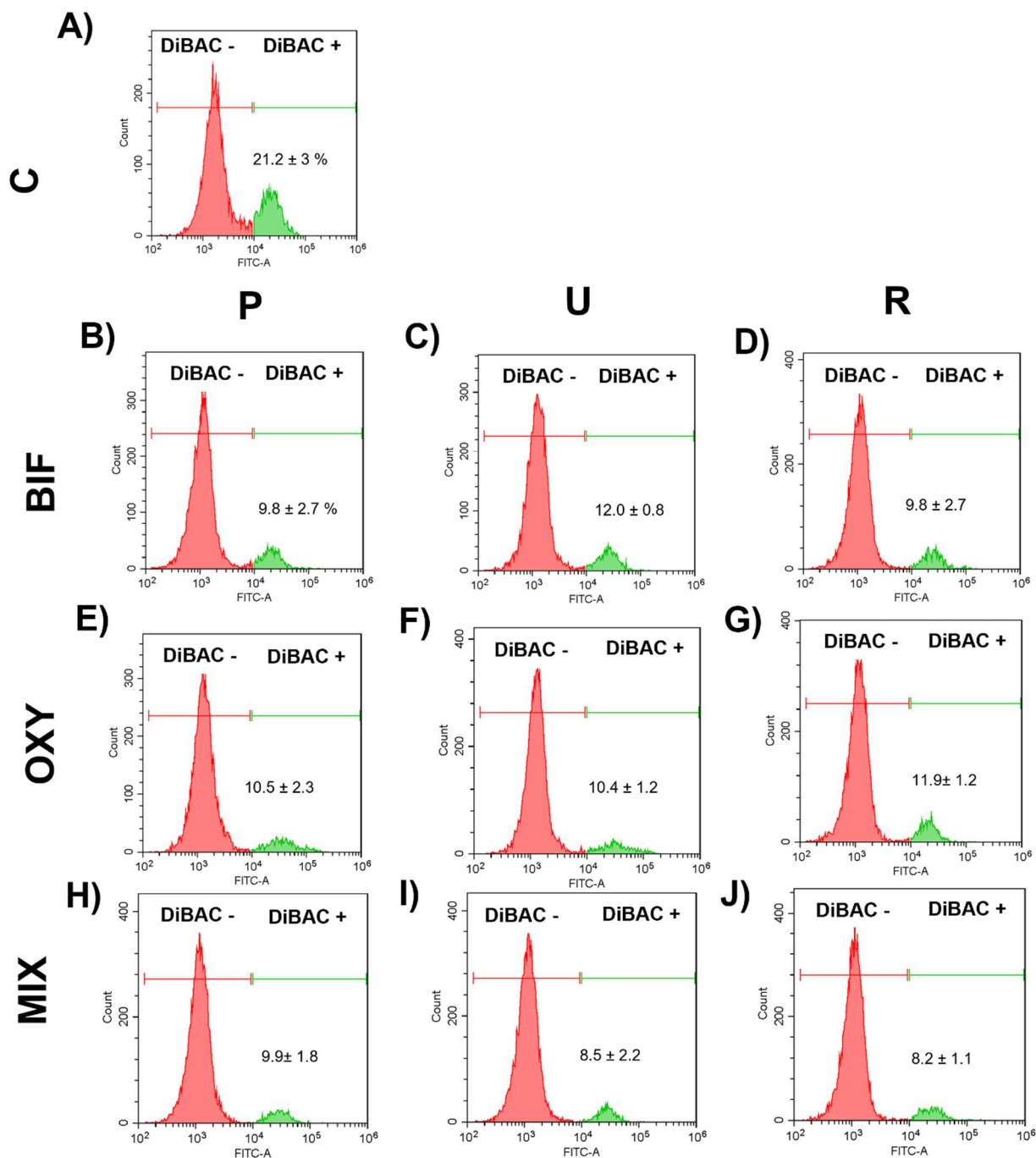


Figure S8. Representative histograms of the DiBAC₄(3) fluorescence in a logarithmic scale, showing the effect on the membrane potential of *C. reinhardtii* of the leachates released from pre-exposure of pristine (P) agricultural plastics to BIF (B), OXY (E), and MIX (BIF+OXY) (H); agricultural plastics in use from farmland (U) to BIF (C), OXY (F) and MIX (I); and agricultural plastics abandoned in a riverbed to BIF (D), OXY (G), and MIX (BIF+OXY) (J). The exposure time of the leachates to the organism was 72 h. (A) represents the ROS (H₂O₂) production in control cells (untreated cells). Y-axis represents fluorescence intensity in arbitrary units and X-axis the fluorescence intensity in arbitrary units. Values are shown as mean \pm SD of the percentage of DHR123+ cells (n = 3, n = 6 control).

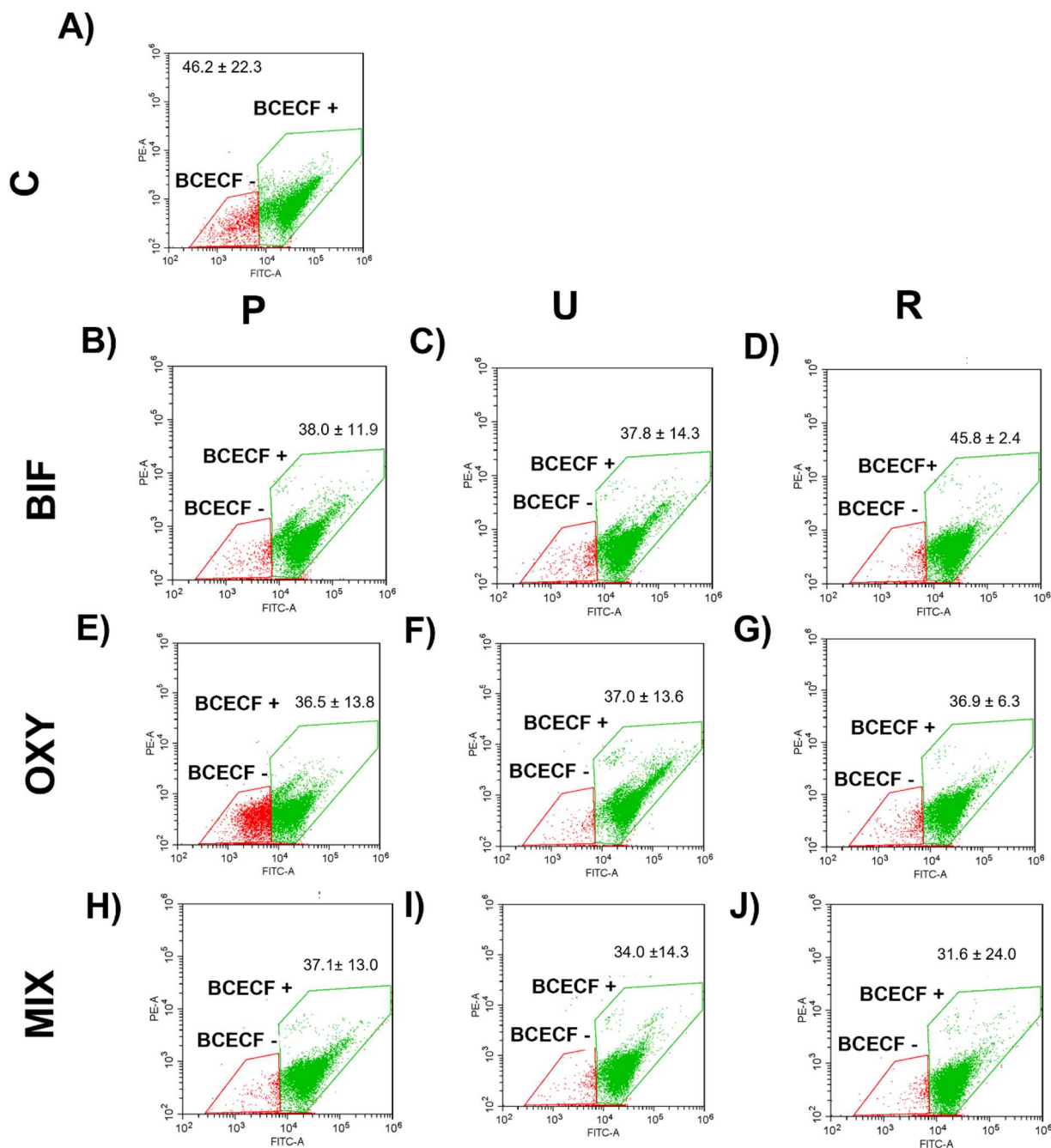


Figure S9. Representative dot plot of the BCECF fluorescence in a logarithmic scale, showing the effect to intracellular pH of *C. reinhardtii* of the leachates released from pre-exposure of pristine (P) agricultural plastics to BIF (B), OXY (E), and MIX (BIF+OXY) (H); agricultural plastics in use from farmland (U) to BIF (C), OXY (F) and MIX (I); and agricultural plastics abandoned in a riverbed to BIF (D), OXY (G), and MIX (BIF+OXY) (J). The exposure time of the leachates to the organism was 72 h. (A) represents the ROS (H_2O_2) production in control cells (untreated cells). Y-axis represents fluorescence intensity in arbitrary units and X-axis the fluorescence intensity in arbitrary units. Values are shown as mean \pm SD of the percentage of DHR123+ cells ($n = 3$, $n = 6$ control).

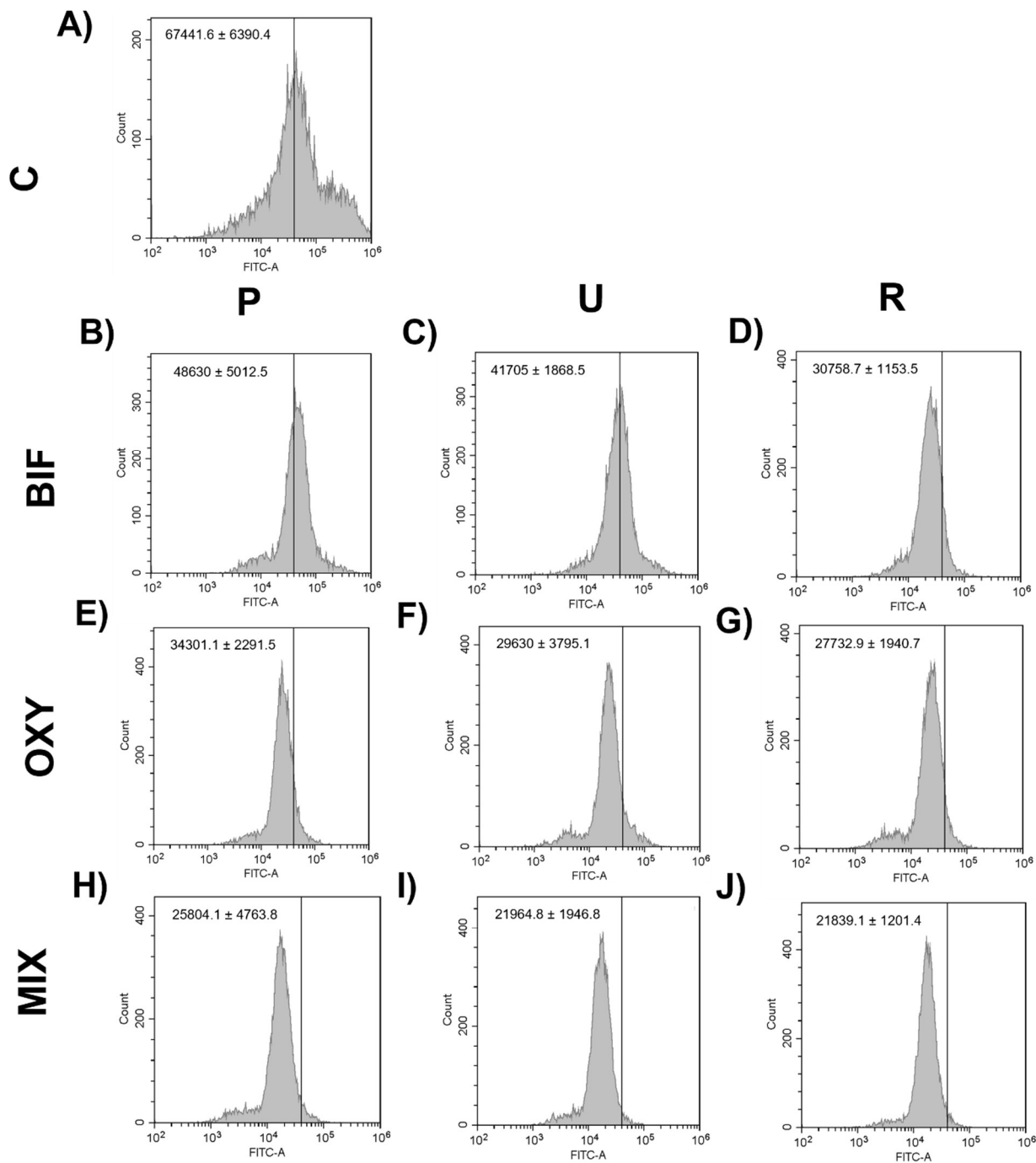


Figure S10. Representative histograms of the distribution of FDA fluorescence in a logarithmic scale, showing the effect on the metabolic activity of *C. reinhardtii* of the leachates released from pre-exposure of pristine (P) agricultural plastics to BIF (B), OXY (E), and MIX (BIF+OXY) (H); agricultural plastics in use from farmland (U) to BIF (C), OXY (F) and MIX (I); and agricultural plastics abandoned in a riverbed to BIF (D), OXY (G), and MIX (BIF+OXY) (J). The exposure time of the leachates to the organism was 72 h. (A) represents the ROS (H_2O_2) production in control cells (untreated cells). Y-axis represents fluorescence intensity in arbitrary units and X-axis the fluorescence intensity in arbitrary units. Values are shown as mean \pm SD of the percentage of DHR123+ cells ($n = 3$, $n = 6$ control).